LUAT
Lehrstuhl für Umweltverfahrenstechnik und Anlagentechnik
Univ.-Prof. Dr.-Ing. habil. K. Görner

UNIVERSITÄT DUISBURG ESSEN
Offen im Denken

Masterarbeit

zur Erlangung des akademischen Grades des

Master of Science (M.Sc.)

im Studiengang Maschinenbau
mit der Vertiefungsrichtung Energie- und Verfahrenstechnik

„Konzeption, Bau und Test eines Reaktors zur CO_2-Abscheidung aus Rauchgasen“

„Assembly and test of a carbonator reactor for CO_2 capture from flue gases “

Ersteller: Parmaksiz, Hazal
Matrikelnummer: 3021164
1. Betreuer: Univ. -Prof. Dr. -Ing. habil. Klaus Görner
2. Betreuer: Dr. -Ing. Gerd Oeljeklaus
Datum: 19. Juli 2022

Versicherung an Eides Statt

Ich, **Parmaksiz, Hazal, 3021164** erkläre hiermit an Eides statt, dass ich die vorliegende Arbeit selbständig verfasst und dabei keine anderen als die angegebenen Hilfsmittel benutzt habe. Sämtliche Stellen der Arbeit, die im Wortlaut oder dem Sinn nach Publikationen oder Vorträgen anderer Autoren entnommen sind, habe ich als solche kenntlich gemacht. Die Arbeit wurde bisher weder gesamt noch in Teilen einer anderen Prüfungsbehörde vorgelegt und auch noch nicht veröffentlicht.

Köln, 19. Juli 2022 Unterschrift:_____

Name

Table of Contents

List of Figures

List of Tables

Nomenclature

Acronyms	Explanation
DLR	Deutsches Zentrum für Luft- und Raumfahrt
CaL	calcium looping
CC	carbon capture
CCS	carbon capture and storage
CCR	carbon capture and reuse
TCES	thermochemical energy storage
FB	fluidized bed
DFB	dual fluidized bed
TGA	Thermogravimetric Analyzer
GC	gas chromatograph
CaO	calcium oxide
$CaCO_3$	calcium carbonate
CO_2	carbon dioxide
O_2	oxygen
CO	carbon monoxide
H_2	hydrogen
N_2	nitrogen
FeCrAl	iron-chromium-aluminum

1 Introduction

The impact of humanity's excessive consumption and inconsiderateness towards the world since the industrial era provoked a global climate change. Rising temperatures of the atmosphere, melting of polar ice caps and rising sea levels, species extinction and meteorological phenomena are only one part of the consequences caused by the immoderate emission of greenhouse gases. To avoid further disasters the need to act urgently is immense. The world is concentrating on renewable energies as a forward step to emit zero greenhouse gases. This however is not possible in very near future but is considered as a long-term plan.

Carbon capture and storage (CCS) holds a huge potential to drastically reduce the emission of carbon dioxide (CO_2) into the atmosphere immediately. Calcium looping (CaL), a cyclic carbon capture process, is one of the carbon capture technologies, utilizing naturally occurring carbonate as sorbent which is cost effective and easily accessible. Existing power plants can be conveniently retrofitted with a CaL system, and future power plants designed with full and partial oxidation reactor.

Worldwide research was boosted and scale up processes already initiated, though still being in a pre-commercial stage. For this reason, this research extends the knowledge on the calcium looping processes, showcasing the potential of a new kind of carbonator in lab-scale size. It offers valuable design and construction data, the studies of the parameters, a guideline on how to conduct the experimental campaign and finally offers valuable data coming from that experimental campaign. It is intended to initiate an upscaling process of this carbonator in the near future, to study the behavior of the system in a large scale to make it ready for the use in power plants. Before this, the carbonator which will be presented here, has to go through several experiments and improvements, to have the system running and to reach maximal efficiencies.

1.1 Motivation

"Net Zero" by 2050 is the target by a steadily growing number of countries, aiming to have a net-zero greenhouse gas emissions by 2050. [1] Focusing on renewable energies is a critical step to achieve this goal. These approaching global climate targets however cannot be achieved only by focusing on renewable energies. In a long-term plan, fossil fuel power generation must be replaced with renewable energies, however, action must be taken quickly, to meet these objectives. Since today's global electricity output still accounts 37 % through coal-fired power generation all over the world and it is yet the cheapest way to produce energy, it will most likely not be abolished in close future.[2] Hence, the reduction of greenhouse gases from the power generation sector through CCS to reach a large-scale reduction of CO_2 emissions as quickly as possible as well as an economical and safe way to achieve these goals, is necessary. Dr. Julio Friedmann, a leading thinker on CCS technologies, is convinced that 15 – 20 % of the global emissions can be handled by CCS, since there aren't many options to address the emissions from the industrial sector. [3]

There are two main leading post-combustion CO_2 capture technologies, that are most probably to be commercialized in the next few years. These are the amine absorption using amine as solvent to absorb the CO_2 out of the flue gas and the oxyfuel combustion, where coal is burnt with a mixture of oxygen (O_2) and CO_2. Even though both technologies are in a mature state, they are still related to several problems. Amine absorption comes with high costs of the solvent, the degradation of the sorbent at high temperatures and a required large amount of heat for the solvent's regeneration. Oxyfuel combustion demands rigorous safety requirements, fouling, leaks affecting CO_2 purity, and an impairment of energy efficiency of around 10 % during CO_2 capture from power plants. In the meantime, the focus has been shifted to new alternatives. [4]

Calcium looping, is one of the most promising carbon capture technologies, offering several advantages, namely a large carbon capture efficiency, potential to implement in large scale power plant facilities, the sourcing of extremely cheap sorbent, and the opportunity for the integration in the cement industry yet still in a pilot and pre-commercial stage. [5]

The calcium looping process offers a variety of application possibilities besides CaL as a carbon capture technology, such as a thermochemical energy storage (TCES) in concentrating solar power plants. While the sorbent in the CaL process in industrial power plants aims for high capture efficiencies and concentrates on the sorbent's performance, the limestone utilized for the TCES process can be used without additional pretreatment and usually lasts longer before degradation. Both technologies are combined in this project.

1.2 The CALyPSOL Project

The Deutsches Zentrum für Luft- und Raumfahrt (DLR) is the research center for aeronautics and space of Germany. The center executes research and development activities in the fields of aeronautics, space, energy, transport, security, and digitalization. Also, the German Space Agency is a part of DLR, where plans for the national space program are implemented on behalf of the federal government. The vision of the DLR institute of Future Fuels, which emerged from the institute of Solar Research, is to develop technological solutions for harvesting large amounts of solar energy in the sunbelt regions of the earth and use it together with the renewable resources, water, and air, to produce fuels cost efficiently.

CALyPSOL (CAlcium oxide LooPing through SOLar energy) (Figure 1.1) is one project of the institute and aims at the separation of CO_2 rich waste gas by a solar driven calcium carbonate /calcium oxide cycle. Two reactors are needed for the cyclic process. Lime (CaO) is first produced from limestone ($CaCO_3$) at temperatures around 900 °C in a calciner reactor using concentrated solar energy. The produced CaO is then used as a sorbent in a second carbonator reactor to capture CO_2 from flue gases. CALyPSOL shall demonstrate the complete CaO cycle. The cycle is characterized by an endothermic reaction (calcination) producing lime, and an exothermic reaction (carbonation) forming limestone again by binding CO_2.

One part of this project is the rotary kiln carbonator, which will be the focus of this work.

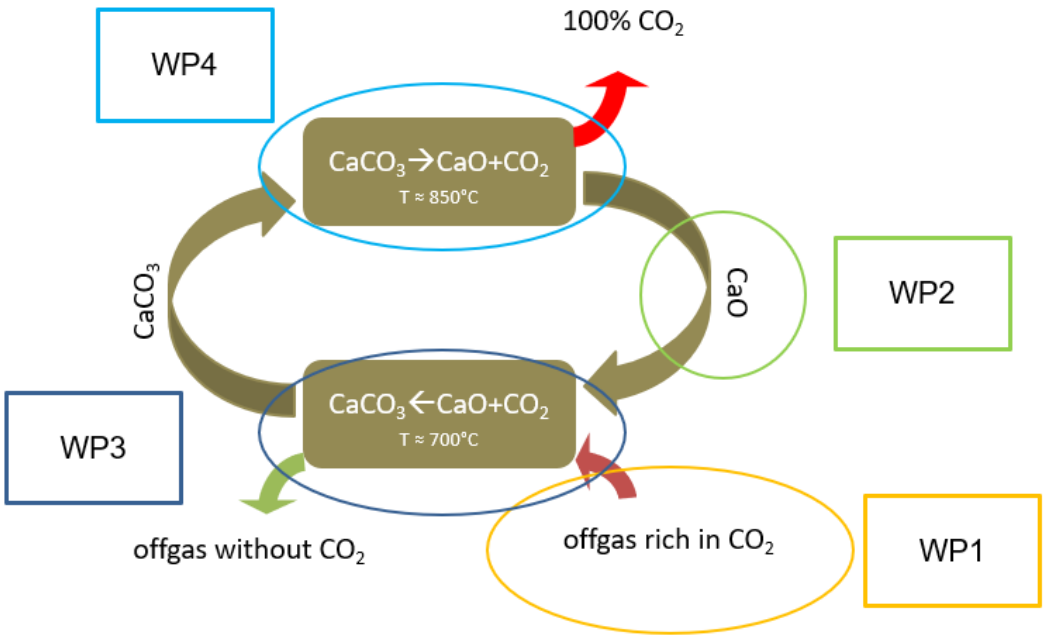

Figure 1.1 Calcium looping cycle and corresponding work packages

First proposed in 2018 with a duration of three years, the whole project was divided into four work packages as seen in Figure 1.1. As this work is part of WP3, the structure, content and targets of this work package will be presented in the following section.

1.3 Scope

Currently there are several pilot and test facilities around the world with a thermal energy demand of a few megawatts, proving the successful implementation of the CaL cycle as retrofit, however, still facing many issues. Thus, the request of enhancement and growing knowledge is grant with a curiosity of innovative and new technologies in this field.

As existing technologies for carbonation such as fluidized bed reactors or entrained flow reactors were developed and improved over the years and are in the pre-commercializing stage, other technologies such as the rotary kiln reactor as a carbonator have hardly been researched, even though holding a great potential.

For this reason, this work offers new insights into the calcium looping process, showcasing a rotary kiln carbonator, which was set up in a lab-scale system and was tested during the projects period.

Conditions for the experimental campaign will be defined, to proof the system's operability, while variables will be adjusted, to achieve the highest CO_2 capture efficiency. This work presents a new approach and offers data, for further investigations and eventually initiating a scale-up of the system to study the behavior in a larger scale, the pre-commercial stage, before actual implementation plans in power plants are envisaged.

1.3.1 Objectives, methodology, and structure of the work

This proposed master's thesis focuses on the construction and test operation of the carbonator. The project for the thesis was divided into three stages. Firstly, the realization of the whole set up. Next, defining operation conditions. And lastly, investigating the operation conditions through an experimental campaign. Major preparations needed to be done for the reactor. All the required components needed to be collected, which included ordering pieces as well as building support structures, e.g., for the screw feeder. Once all pieces were available, the carbonator had to be mounted together, followed by the installation of all the components, to assemble the experimental setup and create a working system.

After realizing the setup, crucial parameters needed to be investigated and operational conditions defined. These are gas temperatures, temperature profiles along the reactor, the inlet mass flow of the particles, the inlet mass flow of the gas and the concentration of CO_2 inside the gas mixture, the rotational speed of the reactor as well of the screw feeder and the angle of inclination of the reactor. As soon as this step was done, experimental conditions were defined in the test's experimental campaigns including the cold tests, the hot tests, and the chemical tests. In order to make statements about the systems efficiency, parameters were modified during the experimental campaign.

2 State of the art

In this chapter current technologies of the carbon capture process are presented. Calcium looping which falls under the category of post-combustion will be displayed in detail. In addition, a detailed overview and analysis of existing calcium looping facilities, projects, and research worldwide was conducted in a chronological order. The balance of the chemical reaction will be portrayed in detail. Moreover, ruling carbonator reactor designs are presented.

2.1 Carbon capture and storage or reuse

The process of removing CO_2 from emission sources is defined as carbon capture (CC). Its purpose is to limit the release of CO_2 emissions into the atmosphere by capturing the CO_2 and then storing it safely.
Carbon capture and storage or reuse (CCS/CCR) consists of these three main steps:

- Capturing the CO_2 from the flue gases or separating the CO_2 from the fossil fuels
- treatment and transport of the CO_2 to a place of further use
- storage or utilization of the CO_2 [6]

It is widely agreed that significant emission reductions are needed in the energy- and carbon-intensive industrial sectors. In some sectors theoretical efficiency limits cannot be reached and process-linked emissions are unavoidable. For this reason, CCS appears as the only available option to reduce direct emissions from industrial processes in a long-term plan.
Equipping the power plants and facilities with the CCS technology is reasonable since the emission is avoided where it originally arises. Three different CO_2 separation approaches are applicable for power plants using fossil fuels.
(Figure 2.1)

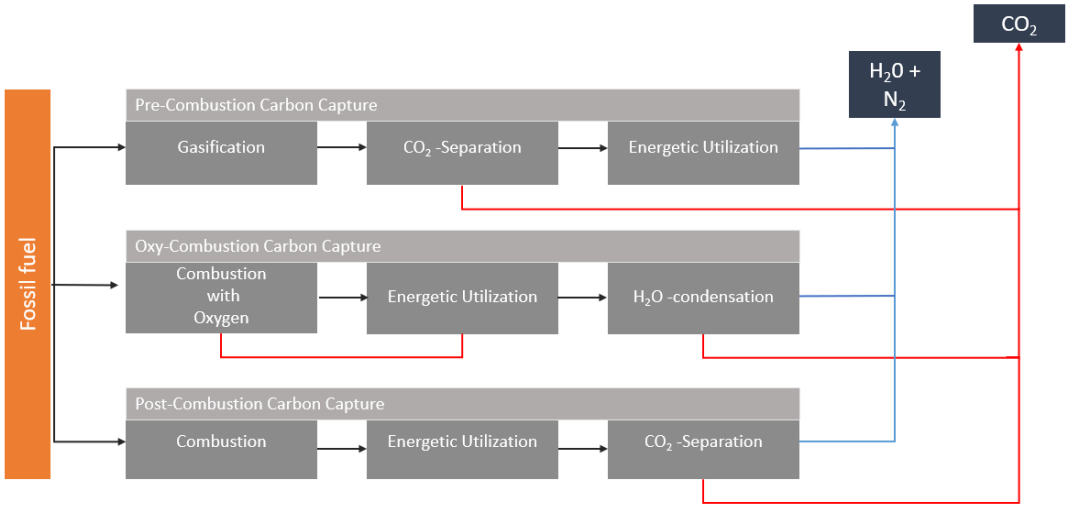

Figure 2.1 Schematics of the three different CO_2 separation processes [6]

Pre-combustion process: This method extracts CO_2 out of the fossil fuel before burning it. A syngas is created by heating the fossil fuel in steam and oxygen. The syngas consists of hydrogen (H_2), carbon dioxide (CO_2), and carbon monoxide (CO). Afterwards a step where only H_2 and CO_2 are present, follows. H_2 can be used for the energy production process, while CO_2 can be isolated, captured and sequestered for further applications.

Oxyfuel combustion process: This process uses pure oxygen rather than air for combustion of fuel or coal. The resulting exhaust gas consists mainly of CO_2 and water vapor. By cooling, the water vapor is condensed and separated from the remaining flue gas. In further steps the flue gas is purified by removing accompanying substances such as SO_2 and a high purity CO_2 stream is produced.

Post-combustion process: CO_2 is typically produced once the fossil fuels are burned to create energy. The resulting flue gases are cleaned by various processes, to separate dust, sulfur oxides, and nitrogen oxides. The purification of the remaining flue gas can be carried out through gas scrubbing in a wet-chemical state where CO_2 bounds to the cleaning agent. When this scrubbing liquid is heated, it releases the pure carbon dioxide again. The detergent is thus regenerated and can be recirculated. Other processes include dry adsorption, in which the CO_2 is adsorbed onto solids, or membrane technologies, in which a gas mixture is separated via a membrane. [6]

2.2 Calcium looping

Calcium looping falls under the post-combustion process and aims to remove CO_2 from flue gases which are emitted from power and industrial facilities by using the sorbent CaO. CaL is based on the cyclic carbonation and calcination of this sorbent. The reaction starts once the ranged temperature of 650 – 700 °C is reached. CaO reacts with CO_2 from the flue gas and forms $CaCO_3$. In a subsequent reaction, the calcination the $CaCO_3$ is heated up to temperatures above 850 °C until it decomposes to a pure CO_2 stream and solid CaO. The detailed reaction equation is discussed in the following chapter.

The first approach on extracting CO_2 through carbonization in large scale power plants was introduced by Hirama [7] and Shimizu [8]. They proposed the removal of CO_2 from flue gas using two fluidized bed reactors which are connected by solid transportation lines. Dry flue gas with a volumetric CO_2 content between 4 - 15 % is conducted in the first reactor, the carbonator. The exothermic carbonation reaction leads to the capture of CO_2 in which $CaCO_3$ is formed. The $CaCO_3$ is then directed into the second reactor, where the endothermic calcination reaction forms CaO back as well as a CO_2 rich gas stream, which can be used for further applications. This was a milestone in the research of extracting CO_2 from flue gases, since a model to remove CO_2 through carbonation was first elaborated. Further investigations were based on these findings and since then, major developments were achieved in terms of large-scale applications. Over the past few years, several institutes and universities started building CaL test facilities as retrofits to existing fossil fuel-fired power generation systems, rather than focusing on building innovative CO_2 neutral power plants. [9]

The following Table 2.1 gives an approximate overview of the CaL test facilities around the world over the past few years. Some of the facilities will be presented afterwards, whereby the different reactor types and designs will be evaluated in the following subsection of this chapter.

Table 2.1 Chronology on CaL research & projects

Year	Research Team & Country	Facility
2004	J.C. Abanades – CSIC (Spain); Edward J. Anthony, Dennis Y. Lu, and Carlos Salvador – CANMET (Canada); Diego Alvarez – INCAR (Spain)	Small pilot fluidized-bed reactor
2009	J.C. Abanades; M. Alonso; N. Rodríguez; B. González; G. Grasa; R. Murillo – CSIC INCAR (Spain)	30 kW pilot dual circulating fluidized bed reactor
2010	A. Charitos; C. Hawthorne; A.R. Bidwea; S. Sivalingamb; A. Schuster; H. Spliethoff; G. Scheffknecht – IFK (Germany)	10 kW dual fluidized bed reactor
2010	W. Wang; S. Ramkumar; S. Li; D. Wong; M. Iyer B.B. Sakadjian; R. M. Statnick; L.S. Fan – OHIO State University (USA)	120 kW entrained bed carbonator, a rotary kiln calciner and bubbling fuidised-bed hydrator.
2011	C. Hawthorne; H. Dieter; H. Holz; T. Eder; M. Zieba; G. Scheffknecht – IFK & EnBW Kraftwerke AG (Germany)	200 kW three fluidized bed reactors (scale up of the existing 10 kW reactor from IFK)
2009 - 2013	A.S. Biezma; J. Paniagua; L. Diaz; M. Lorenzo; J. Alvarez; D. Martinez; B. Arias; M.E. Diego; J.C. Abanades – La Pereda (Spain)	1.7 MW dual circulating fluidized bed reactor
2013	ITRI (Taiwan)	3 kW fluidized bed carbonator & rotary kiln calciner

2013 – 2017	Technische Universität Darmstadt – SCARLET	1 MW – 20 MW dual circulating fluidized bed reactor
2015 – 2018	CO2 capture from cement production CEMCAP (EU)	200 kW three fluidized bed reactors (facility from IFK)
2018	S. Turrado; B. Arias; J.R. Fernandez; J.C. Abanades – INCAR-CSIC	Drop Tube reactor
2016 – 2019	FlexiCaL (EU)	200 kW three fluidized bed reactors (Facility from IFK) Regenerator operated in circulating mode carbonator either circulating mode or bubbling mode
2019	J. Plou; I. Martínez; G. S. Grasa; R. Murillo (Spain)	Solid feeding system & entrained flow reactor and fluidized bed vessel.
2017 - 2020	Clean clinker production by calcium looping process CLEANKER (EU)	Reactors as retrofit of existing cement plant. carbonator is an entrained flow reactor and calciner

Most of the lab- and pilot-scale facilities used fluidized bed reactors to remove CO_2 out of the flue gas. A team of the Carbon Science and Technology Institute (INCAR) from Spain was one of the first to build a test facility in the size of 30 kW composed of two interconnected circulating fluidized bed reactors. [10] The outcome of the experiments with the test facility showed that the carbonator reactor and thus the CaO functions as an effective absorber for CO_2, as long as there is a sufficient bed inventory and solid circulation rate. There are many more institutes and working groups who worked on a test facility to show the efficiency and the advantages of CaL. The Institute of Combustion and Power Plant Technology (IFK) at University of Stuttgart set up a 10 kW lab-scale dual fluidized bed facility consisting of a riser and bubbling fluidized bed. [11]

They managed to demonstrate the CaL process in the kW dual fluidized bed facility, moreover achieving CO_2 capture efficiencies above 90 %. Throughout the whole experiments, parameters were adjusted to achieve the highest efficiency.

Several studies and research teams used the same facility, while focusing on different aspects of the CaL process. Serving as a model, a joint industrial-university research and development project between IFK and EnBW Kraftwerke AG from Germany was launched, to scale up the existing pilot plant to a size of 200 kW. [12] The kW CaL pilot plant had the aim to demonstrate realistic operating conditions while removing CO_2 from real combustion gas as well as improving knowledge on a bigger scale through the guidance of the experimental data.

SCARLET, a project initiated by the University of Darmstadt was one of the most promising projects, spanning couple of years and upgrading a pilot plant in the size of 1 MW to a pilot plant reaching 20 MW. The aim was to provide essential information and tools for the scale-up process of the CaL process. As well as the demonstration of a continuous, self-sustaining operation of a pilot facility. Furthermore, the aim was to provide a technical, economical, and environmental assessment of the CaL process and to offer an expertise for the scale-up as well as the integration of such systems for commercializing. [13]

Over the past few years, the number of projects in the cement production industry rapidly increased, aiming to achieve zero CO_2 emissions utilizing different carbon capture technologies one of them being the CaL-cycle. A few of them are: CEMCAP, FlexiCaL, and CLEANKER.

CLEANKER a project under Horizon 2020 carried out by the cement plant facility in Vernasca (Piacenza, Italy) in cooperation with CLEANKER partners such as Politecnico di Milano (Milan, Italy), Laboratorio Energia e Ambiente Piacenza (Piacenza, Italy), IKN GmbH (Neustadt, Germany), University of Stuttgart, and Verein Deutscher Zementwerke (Düsseldorf, Germany) is one of the ongoing projects aiming to demonstrate an integrated CaL process for CO_2 capture in cement plants. First proposed in 2017 with a span of more than four years due to the pandemic situation, the facility intents to demonstrate the CaL process in a new scale, namely 1300 kt/year. The first two years were focused on a detailed design of the CaL demonstration system, the characterization of raw meals as CO_2 sorbents and the construction of the demonstrator. In October 2020 the pilot plant was first set up and short and long state tests were conducted. [14]

Yet, there is no existing commercialized CaL-system in power plants. However, the growing number of projects and thus the knowledge gained, are an excellent prerequisite and preparation for grant scale CO_2 capture in near future.

2.2.1 Kinetics

Now that the current state of the CaL-process in operation is settled, the chemical balance needs to be clarified, to create a foundation and understanding for the following chapters.

The calcium looping process is based on the reversible carbonation of CaO-based sorbent, mostly derived from limestone. The reaction is displayed in equation (1).

$$CaO(s) + CO_2(g) = CaCO_3(s) \quad \Delta H_{r,298K} = -178\, kJ/mol \tag{1}$$

The carbonation reaction is exothermic, whereas the backward reaction, the calcination is endothermic.

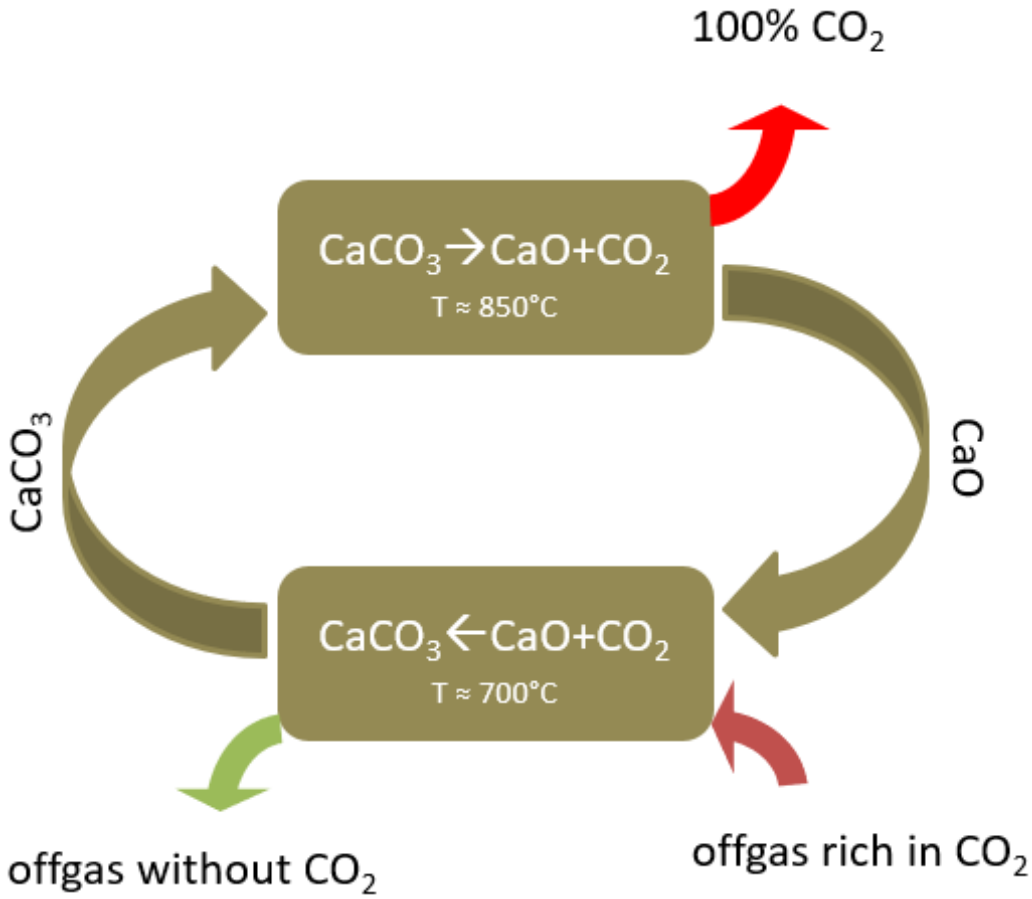

Figure 2.2 Calcium looping cycle

Both reactions operate at very high temperatures, 700 °C for the carbonation and 850 – 900 °C for the calcination, regarding the kinetic and chemical equilibirum. One commoly known concept to determine the equilibrium curve by using equation (1) can be done by using the thermodynamic coefficients provided by McBride et al. [15]

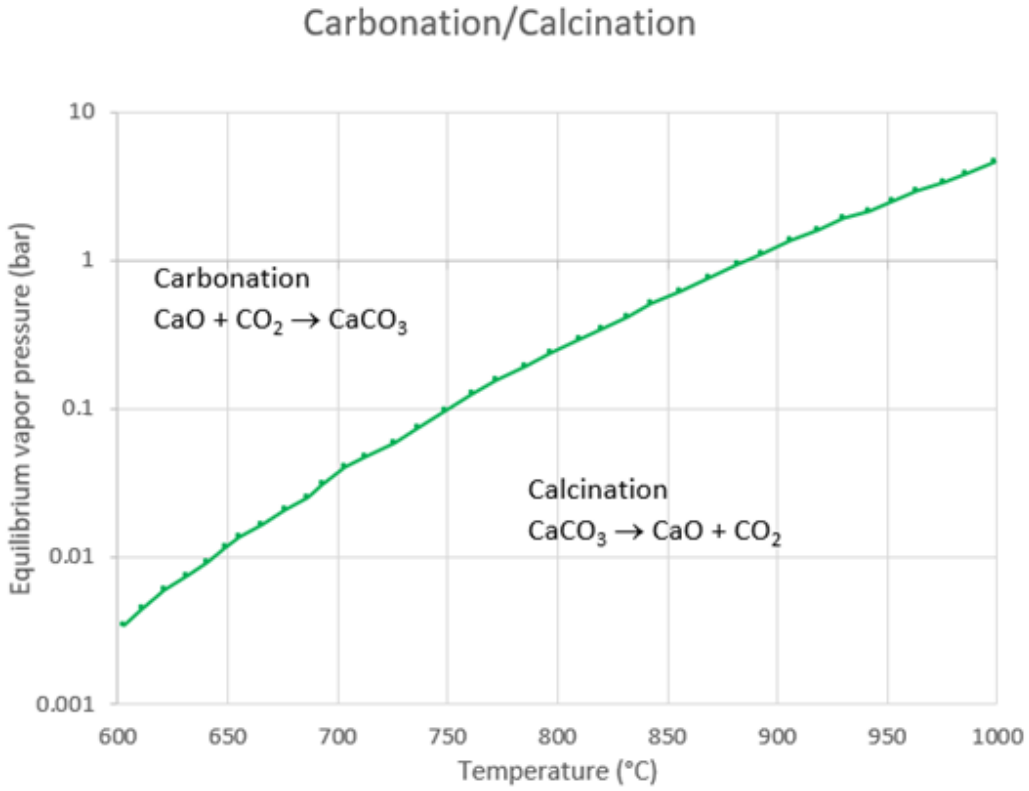

Figure 2.3 Equilibrium vapor pressure of CO_2 over CaO as a function of temperature [15]

The ideal carbonation temperature is between 650 – 700 °C (Figure 2.3) characterized by an initial rapid rate period followed by an abrupt transition to a very slow reaction rate. Choosing the ideal carbonation temperature is a compromisse between a higher equilibrium at lower temperatures and a decreased rate of reaction. The calcination temperature on the other hand is optimal at temperatures of around 900 °C, reacting rapidly and with a higher rates at higher temperatures, however causing a faster degradation of the sorbent. [16], [17]

The degradation of the sorbent, thus the loss in sorbent reactivity, is also caused by the following reasons: sintering of the porous CaO due to the high temperatures, other undesired reactions (such as sulphation and sulphidation), loss of bed material due to abrasion, and ash fouling. [17]

The CaL-cycle demands the sorbent to go through repeated CO_2 capture-and-release cycles. Due to the degradation of the sorbent mentioned before, the cycle is not fully reversible, affecting the capture-efficiency of the cycle. This phenomenon can be explained with the carrying capicity of the sorbent.

The carrying capicity is defined as the maximum conversion rate of CaO to $CaCO_3$ and is known to shrink with the increasing number of cycles the sorbent is running through as seen in Figure 2.4. There are two distinct reaction stages of carbonation. The fast carbonation stage, where the fresh CaO-surface is exposed to the CO_2 and simultaneously reacts and forms a $CaCO_3$ product layer on the surface. Following the slow carbonation stage, due to the diffusion resistance offered by the $CaCO_3$ layer. [18]

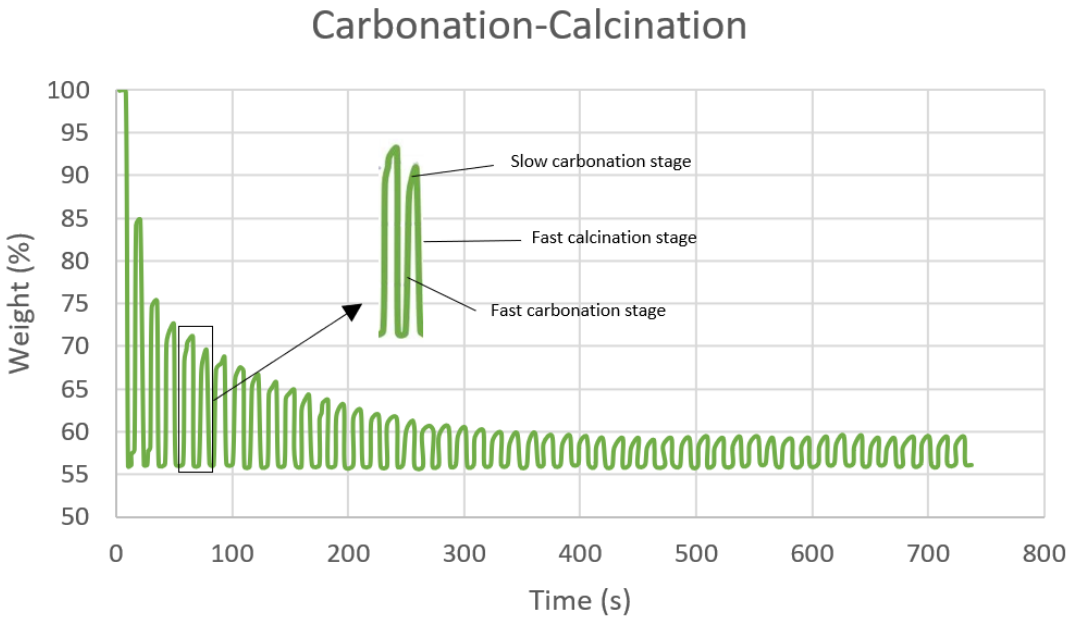

Figure 2.4 Carrying capacity of CaO sorbent through 50 CO_2 capture-and-release cycles represented in terms of mass change vs. time [17]

The sorbent's effiency to capture CO_2 depends on the reactions kintetics, the grain size of the sorbent, the specific surface area of the grain, and the pore space characteristcs. [18]

In order to maintain a steady state, fresh sorbent needs to be added regurlarly.

2.2.2 Reactor design

Different reactor types were presented during the CaL section. This chapter will showcase the existing reactor types and their working principles.

Fluidized bed reactor

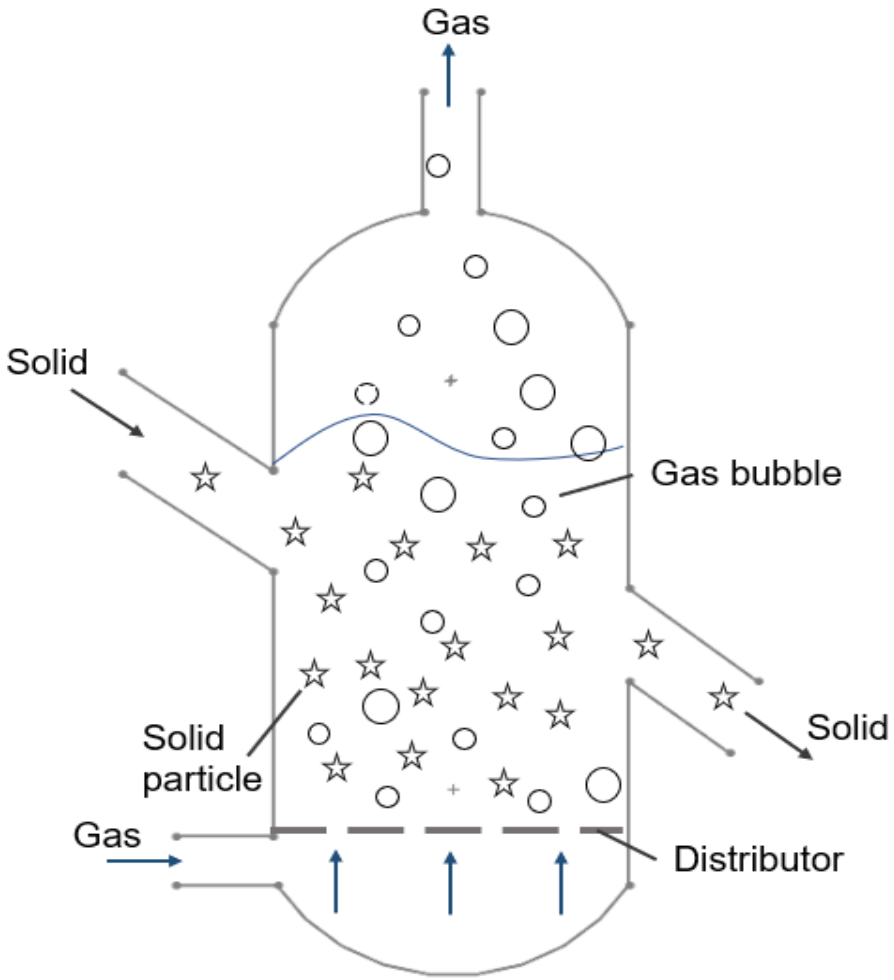

Figure 2.5 Simplified schematic diagram of a FB reactor

Fluidized bed (FB) reactors are fluid-solid reactors where solid particles keep being in motion by an upward gas flow. For this purpose, the gas is passing through a distributor at the lower end of the reactor. The distributor either consists of several nozzles or a distributor plate with many openings.

When starting up the fluidized bed, the gas flows through the particle pile on the distributor plate. The particles get lifted and begin to float in the gas stream when reaching a sufficient high velocity. [19] With respect to calcium looping processes, different kinds of fluidized bed reactors were deployed.

Dual fluidized bed reactor

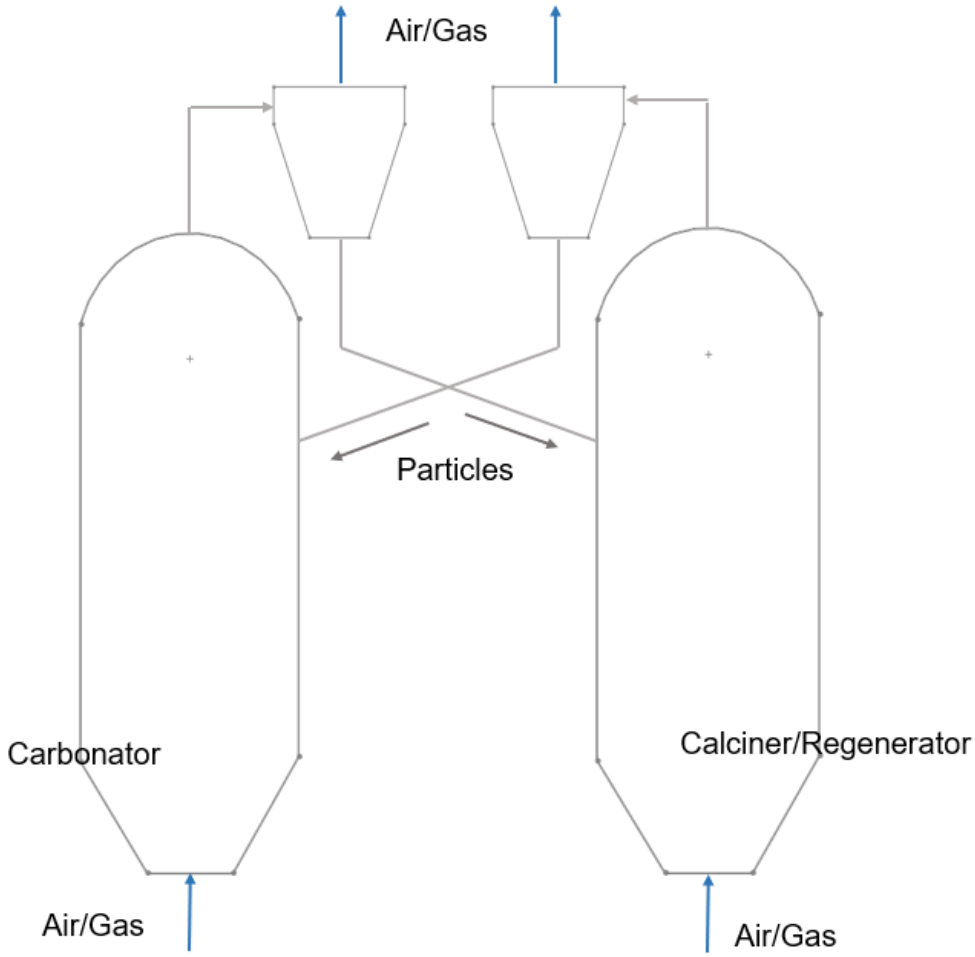

Figure 2.6 Simplified schematic diagram of a DFB reactor

DFB systems consist of two FB interconnected reactors for solid transport. Depending on the application, one reactor corresponds to the carbonator while the other one is either a calciner or regenerator. A regenerator can be any device to release a pure stream of CO_2 inside the reactor. Several lab-scale systems and pilot plants have been constructed over the years, presenting the calcium looping process successfully. One of them was commissioned by the INCAR-CSIC consisting of two circulating fluidized bed reactors: the carbonator and the air-fired regenerator. A mixture of air and CO_2 enters the carbonator, where it reacts with CaO at temperatures between 600 °C and 700 °C. The formed $CaCO_3$ is then treated in the regenerator at temperatures at around 800 °C and 900 °C.[20] Due to the small scale and sintering of the material, the reactors weren't operating with the desired efficiency of the calcium looping process, leading to a short operation time.

However, these dynamic tests with changes in solids circulation rates and bed inventory in the range of minutes were an excellent source of experimental information for validating the process and deriving appropriate reactor models.
With a thermal demand of 1 MW to 20 MW the pilot plant of the Technische Universität Darmstadt (TUD) is one of the biggest DFB systems out there. The main set-up of the reactors resembles to the INCAR set-up, in a bigger scale and with additional components, such as a heat exchanger, a dust filter, and an internal heat dissipation system inside the reactor, which dissipates the heat of the carbonation and sets the desired temperature level. With the systems grant CO_2 capture, efficiencies of more than 80 % were achieved. [21] Other DFB systems were investigated from the Institute of Combustion and Power Plant Technology (IFK) at University of Stuttgart. [11]

Entrained flow reactor

The characteristics of a typical entrained flow are the low solid-to-gas ratio reactor are the brief residence time of solid and gas phase. The residence time can be understood as the time the particles remain inside the furnace and will be addressed in the upcoming chapters. The CaL system consists of three different parts: the solid feeding system, the entrained flow reactor serving as carbonator, and a fluidized bed vessel providing the reactor the required heat. The CO_2 gets mixed up with the sorbent/air mixture and is then introduced to the reactor, where it starts to react within seconds due to the provided heat coming from the bubbling fluidized bed reactor. [22]

Drop tube reactor

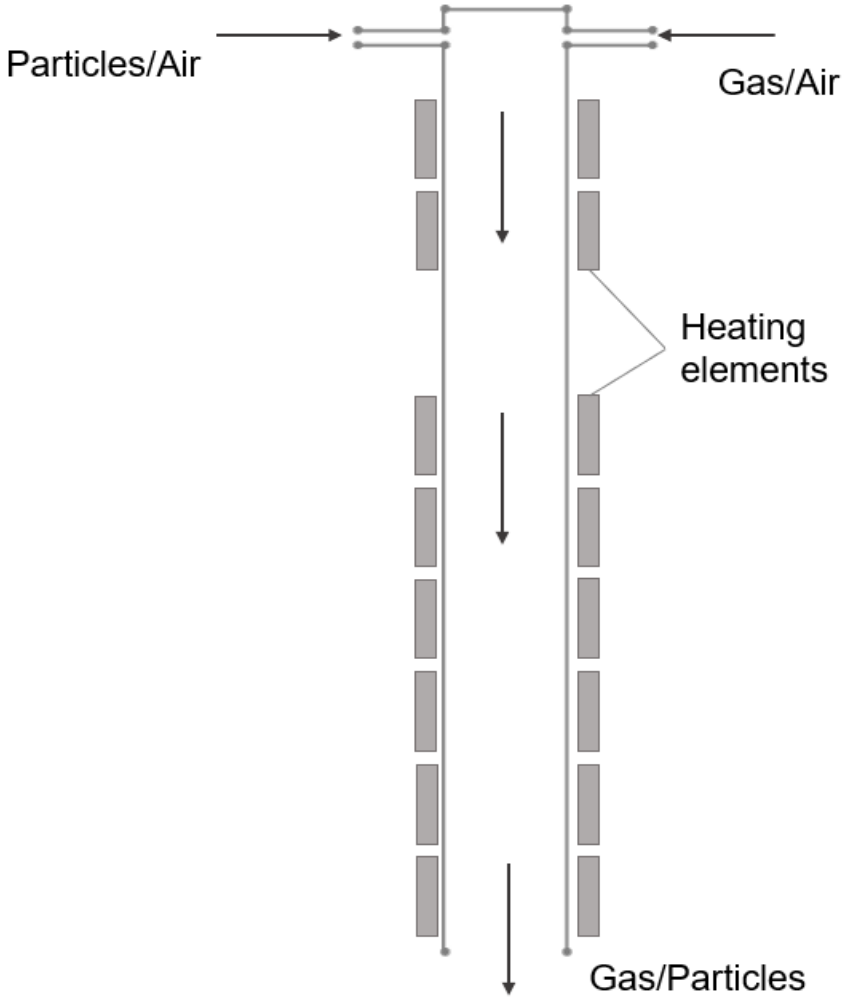

Figure 2.7 Simplified schematic diagram of a drop tube reactor

This kind of reactor belongs to the category of entrained flow reactors and is characteristic for the carbonation of fine CaO particles with few seconds of gas-solid contact, which is required in the cement production industry. A drop tube reactor has been deployed by INCAR-CSIC, investigating integrated CaL systems using entrained bed reactors in the cement production industry. The carbonator is a down-flow reactor, with heating elements installed along it, to maintain a uniform axial temperature. Particles and gas get injected at the top of the reactor and move downward together. The flow is controlled by a vibrating feeding system and the gas by a mass flow controller. While moving downward together, the contact time of particles and gas is around 1 – 5 s. Even though, this reactor was the very first prototype, the results from the experimental campaign were successful, and have demonstrated that the carbonation conversion is dependent on the materials carrying capacity and the CO_2 concentration inside the mixture. [23]

3 Experimental set-up

This chapter focuses on the set-up of the whole carbonator system and each component, which are deployed here. Before going into the set-up, the concept of the carbonator, the main part of the system will be elaborated in detail.

3.1 Design and conception of the carbonator

As the main part of the carbonator, the reactor was designed in a way to ensure and favor the reaction. Already existing projects and designs were investigated, trying to achieve an ideal reactor for high efficiency capture rates. A rotary kiln is commonly used for the calciner of a CaL system, the carbonator usually is either a fluidized bed reactor or entrained flow reactor. The advantages a rotary kiln has to offer can be applied for a carbonator as well, which are: adjustable residence time of particles by controlling the rotational speed of the reactor and the tilting angle, achieving high temperatures in the cavity, continuous solid conversion in controlled atmosphere, uniform radial heating, good heat transfer due to the contact of the rotating particle bed with the hot reactor walls, option of operation in co-current or counter-current flow, which allows heating of particles by the exhaust gas [24], wide range of particle size distribution, adjustable residence time of gas by adjusting gas flow, and less particle abrasion due to the slow rotation. As there is no solid ground on knowledge and research on rotary kiln carbonators, this work will be a milestone, providing information and data for future applications and for the scale-up process. The following Figure 3.1 shows the set-up of the carbonator reactor, which was designed during the projects span-time.

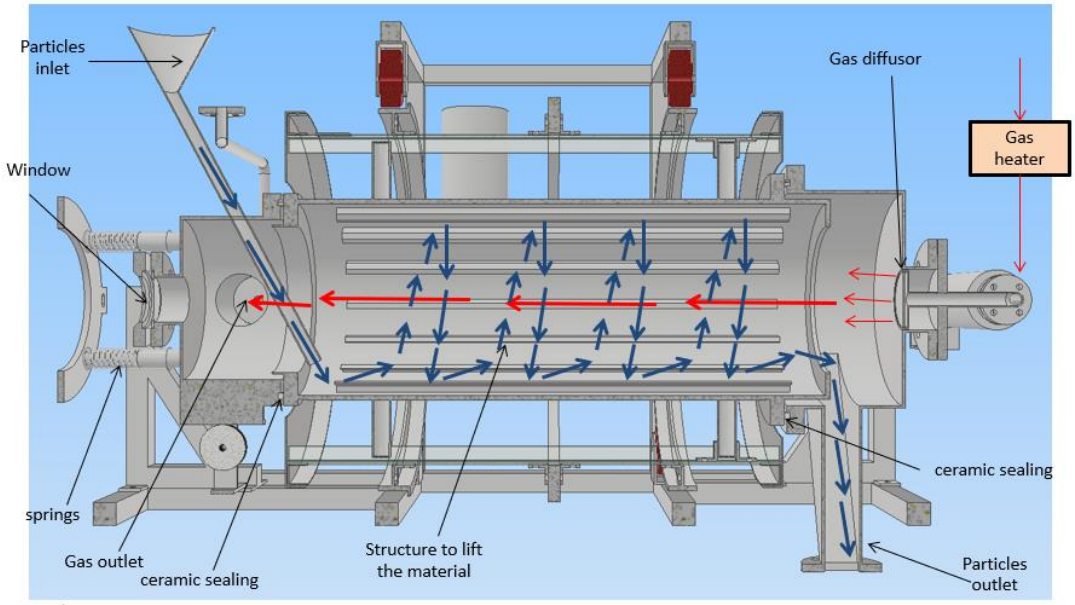

Figure 3.1 CAD drawing of the carbonator with particle flow and gas flow

As already mentioned, the calcium looping reaction is only taking place once a certain temperature level is reached (starting from 650 °C). This condition is crucial, since it determines the design in terms of the material used for the reactor. For this reason, the chosen material needs to withstand temperatures of 1000 °C and even higher, since the temperature input needs to be higher, due to heat losses. Therefore, heat resistant steel (1.4841), which can withstand temperatures of around 1150 °C was used for parts of the carbonator, where high temperatures were expected. The reactor itself is a rotary kiln with shovels attached to the inner wall to guarantee a homogeneous distribution of the material while it rotates. While particles enter from one side, the gas enters from the opposite direction. A screw feeder will feed the particles into the reactor through a pipe, which is fixed on the reactor with a certain angle, to guarantee the particle flow. The carbonator is slightly lifted on the side of the particle flow to ensure the forward movement of the particles inside the reactor. These fall into the storage on the other side of the carbonator. A window is mounted on the particle inlet side, to allow an insight into the reactor, during the experiments. The rotation ensures that the particles get distributed evenly and that each particle faces the flue gas, ensuring a high capture efficiency. While gas is entering the reactor, the system must be gastight. To ensure the tightness, the gas inlet and gas outlet structure exert a certain force/pressure on the reactor.

A spring structure is fixed at the gas outlet side, which can be adjusted, depending on the required force/pressure. Since the reactor is exposed to high temperatures, a bearing withstanding the temperature and the force between the planar faces of the reactor and the gas inlet and gas outlet side is needed. The motion of the reactor is transmitted through a gear set transferring high torques. Four wheels carry the whole reactor, allowing a horizontal movement of the reactor, since the reactor will expand while experiencing heat.

3.2 Set-up of the system

The carbonator consists of several different individual parts that are connected to each other to create a working system. Each of them has a crucial task to enable a reaction at lab-scale. In this chapter, each component will be presented, as well as their role for the whole experimental set-up, which can be seen in Figure 3.2.

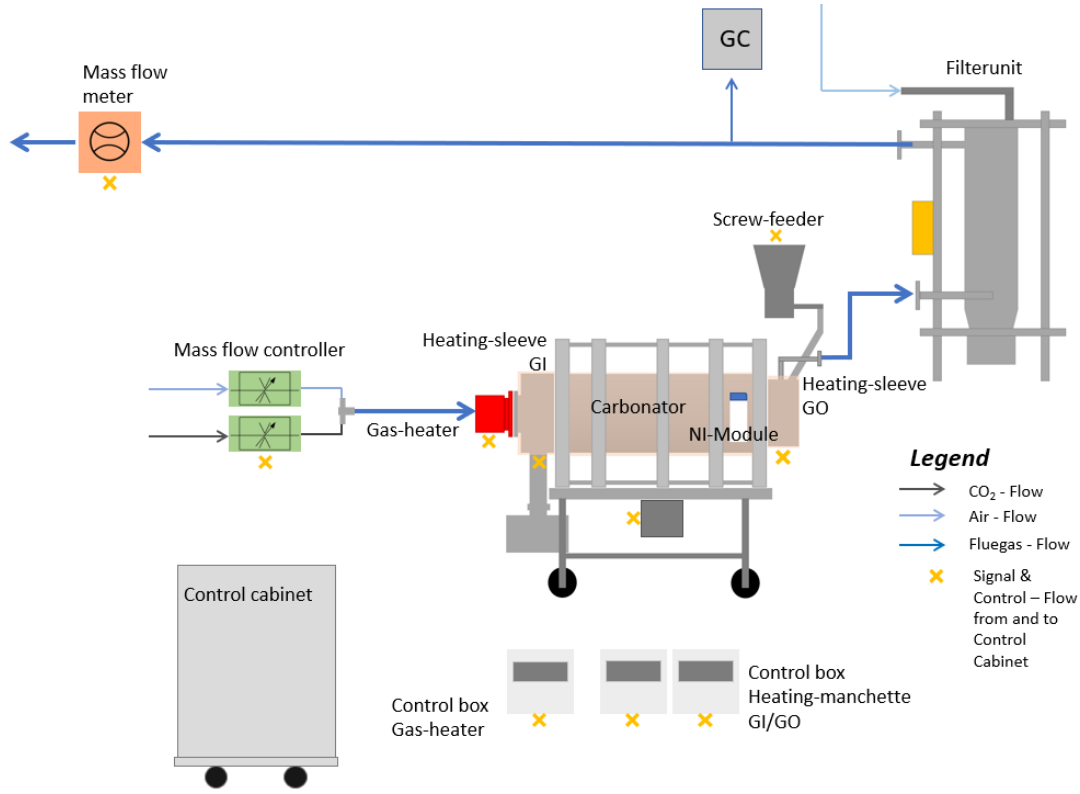

Figure 3.2 Experimental set-up

a) Carbonator

The central part of the carbonator is the reactor, whereby the cylinder is the main part of the reactor, made of heat resistant steel (1.4841). (Figure 3.3) It is the place where the reaction takes place. To distribute the particles evenly inside of the cylinder, shovels with a certain geometry were fixed evenly onto the inner walls of the cylinder. High heat wheels carry the whole cylinder on a frame structure and enhance the rotation. A motor (KEB S22AV DM80K4 TS) with a maximum speed of 1405 1/min is mounted below the reactor and enables the rotation of the carbonator. The motion from motor to reactor is transmitted by two intermeshing gears. There is a gas-inlet and gas-outlet structure, which hold the cylinder in his position.

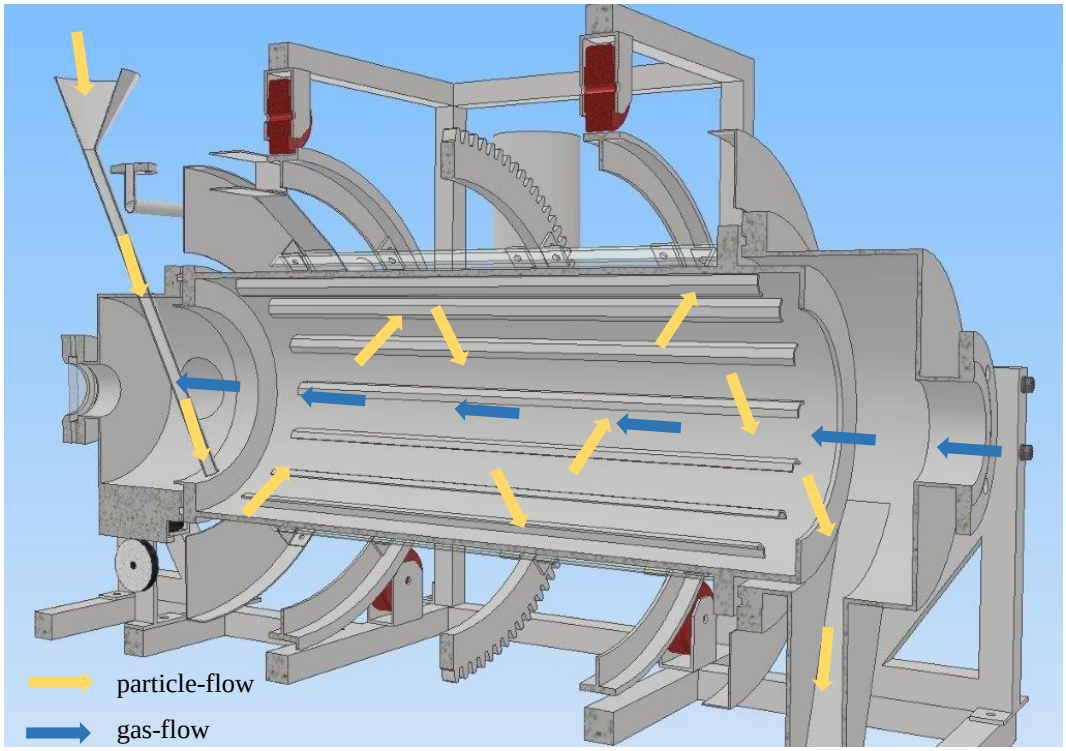

Figure 3.3 CAD drawing of the carbonator with particle- and gas flow

To ensure the rotation, to avoid any wear between the planar faces of the components, and to ensure the gas tightness of the whole system, a cylindrical high heat bearing made of Kelutherm® is placed in between the planar faces. During the reaction, the reactor is heated up to temperatures of around 700 °C. Since steel has the property to expand when getting heated up, a countermeasure to ensure the system is gastight during the whole process must be implied. A pressure plate with springs is fixed at the particle inlet side and exerts a certain force onto the cylinder. The pressure distribution can be adjusted once the reactor expands.

While gas enters the whole system through one end, it exits through the opposite direction through pipes. The particles enter on the opposite side of the gas through a screw feeder.

b) Screw Feeder

The screw feeder (Process Control) as seen in Figure 3.4 is responsible for the particle injection during the experiments. It consists of two parts, the storage, and the feeding unit which are connected to each other.

The storage has a volume of around 15 l and can take up to 10 – 15 kg of $CaO/CaCO_3$, depending on the grain size of the particles. There is a bridge breaker inside the lower half of the storage and just above the screw connected to a motor. It consists of two counter facing paddles on a shaft. Due to the size of the particles, they tend to stick to each other and form a bridge above the screw, preventing a steady flow. The bridge breaker is designed to provide a constant uninterrupted flow of particles.

Figure 3.4 Screw feeder used for experiments

The second part, the feeding unit is responsible for the forward movement of the particles. Depending on the shape and the diameter of the shaft and the blades (Figure 3.5), the particles flow in different manners. Just like the bridge breaker, the screw is also connected to a motor, ensuring the rotation of it.

Figure 3.5 Screws with varying diameter

Both motors are connected to two individual frequency convertors (Siemens Micromaster 420) inside the control cabinet, to control and set the input speed of the motor. (Figure 3.6)

Figure 3.6 Siemens Micromaster 420 Frequency converters

The connection between screw feeder and reactor must be flexible, due to the expansion of the carbonator once it reaches high temperatures. Therefore, a fitting metal below was used, which is visible in Figure 3.7. The metal below can be stretched a few centimeters in both directions.

Figure 3.7 Flexible connection of screw feeder and reactor

c) Heating components

While particles enter at one side of the reactor, the gas enters from the opposite direction. The gas enters though a gas heater (KANTHAL), which can heat gas up to 1200 °C. (Figure 3.8) The core of the gas heater consists of a heating coil made of an Iron-chromium-aluminum (FeCrAl) heating wire, which is wound around a ceramic rod and then inserted into a quartz tube.

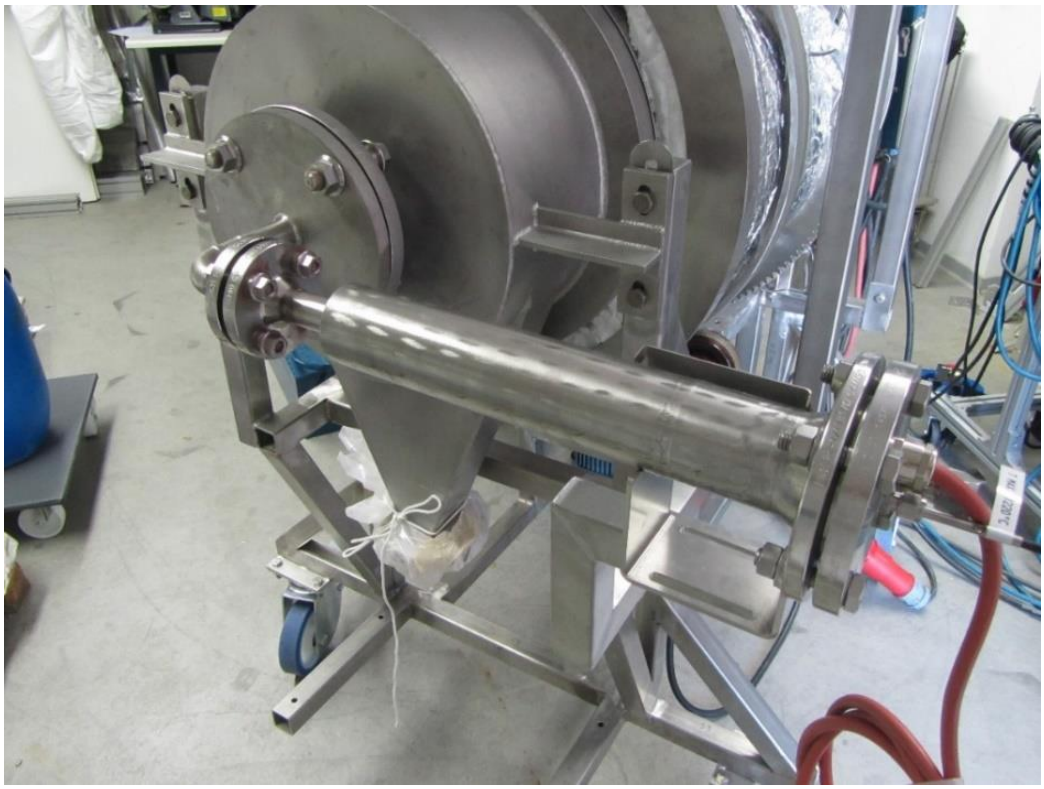

Figure 3.8 Gas heater from Kanthal

Since steel is inert, the wall temperature increases slowly. Therefore, more power to achieve the required temperature and enable the reaction is needed. The cylinder is covered with a mineral insulated heating cable (Isoheat), which can be heated up to 1000 °C and is responsible for the main heat supply. This heating cable will only be used during the preheating process and will be disconnected before starting the rotation of the cylinder. The cable is connected to the power supply of the room and has to be unplugged, once an appropriate temperature is achieved. Two heating sleeves (Isoheat) are wrapped around the gas-inlet and gas-outlet structure, to speed up the whole heating process. These can be heated up to temperatures of around 900 °C. (Figure 3.9)

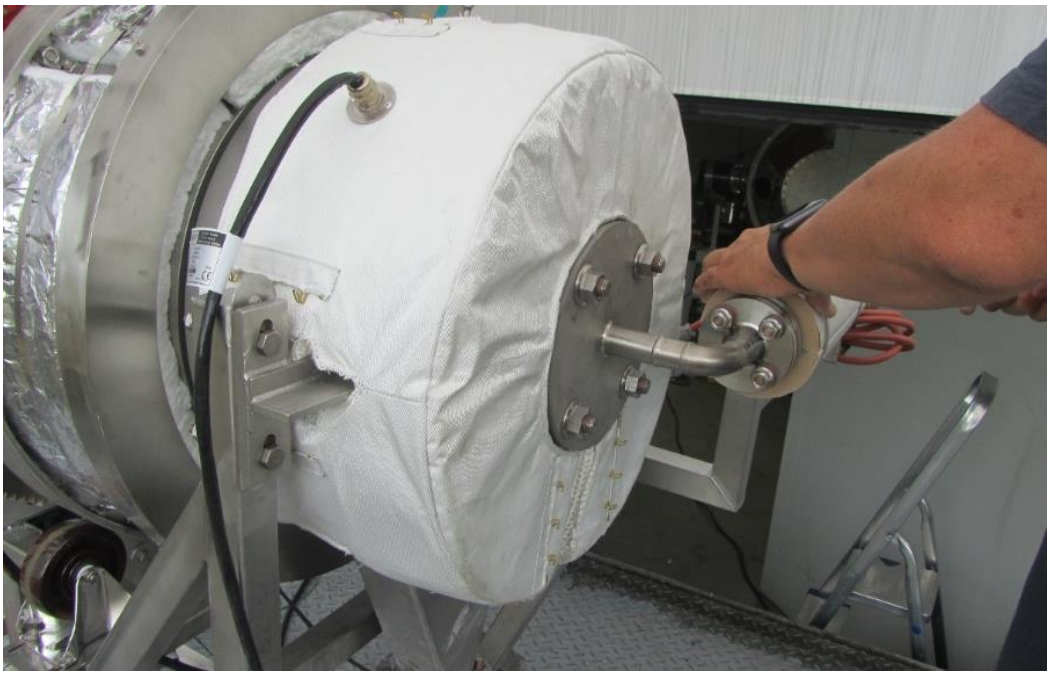

Figure 3.9 Heating sleeve from Isoheat

All the heating elements are connected to an individual control unit, (Horst HT MC11) (Figure 3.10) which monitors the current temperature of the elements and regulates it based on the input. These control units are connected to the control cabinet, to monitor and regulate every device using one universal control interface. The control cabinet will be introduced in the following section.

Figure 3.10 Control boxes for heating elements from Horst

To prevent a major heat loss during the testing phase, the reactor is covered with two layers of Superwool Plus and one layer of Firemaster Marine Plus insulation material (Morgan Thermal Ceramics), each with a thickness of 50 mm, resulting in a total thickness of 150 mm. (Figure 3.11) The final thickness of insulation was determined from thermal balance calculation, during the design stage of the reactor.

Figure 3.11 Reactor with second layer of insulation material

d) Mass flow controller

The composition and velocity of the input gas has to be regulated, therefore mass flow controllers are required. There are two mass flow controllers from the company MKS, (Figure 3.12) one which regulates the flow of atmospheric air (GM100A008105F5MV020) and one for the CO_2 stream (GE50A025384F5V020). The two individual streams will be combined with a T-plug-in connection, resulting into a single gas flow, before entering the reactor. The stream enters the system through the gas heater, where the gas mixture gets heated up for the further process. Depending on the aspiring CO_2 content in the mixture, the velocity of the streams must be fixed.

Figure 3.12 Mass flow controller from MKS

e) Filter Unit

To avoid that fine particles remain in the gas, a filter has been installed after the carbonator. (Figure 3.13) After the reaction takes place, the gas leaves the system through a flexible metal pipe, which is connected to the filter unit, operating with pressurized air. The system includes filter candles, which have a certain size, chosen according to the size of the particles. Once, the candle is clogged, the pressure inside the system will increase, reaching the pressure triggering the impulse air blast cleaning the filter candle.

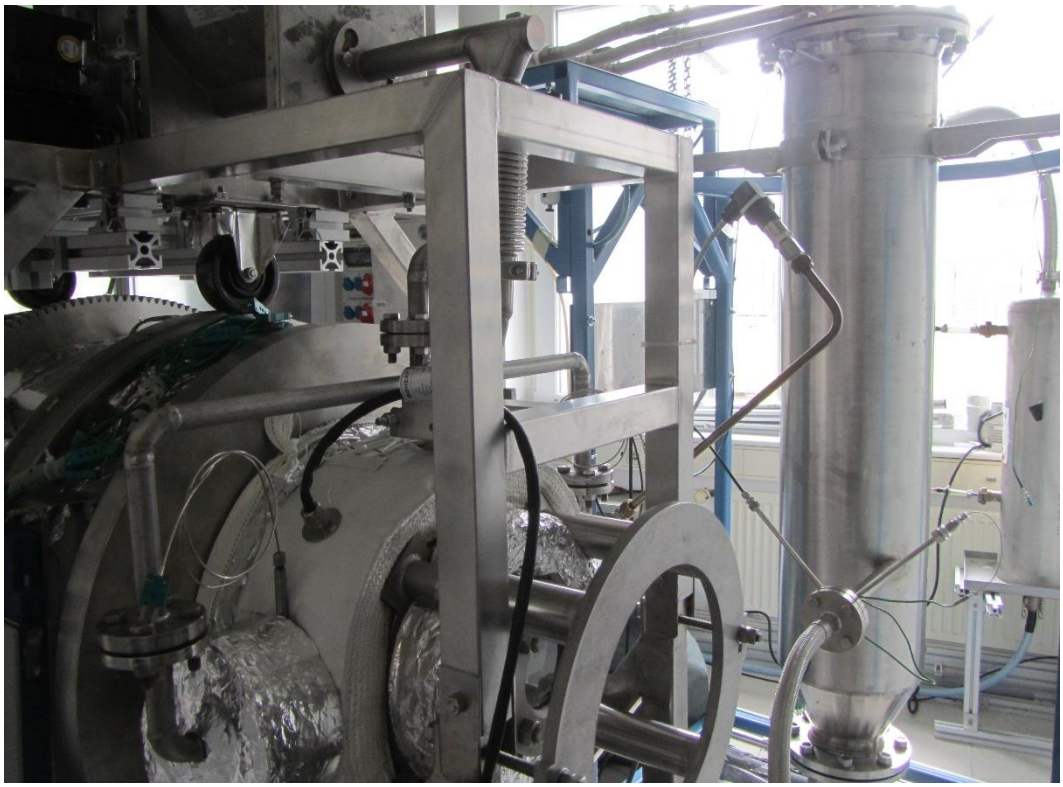

Figure 3.13 Carbonator connected to the filter unit

f) Monitoring components

Temperature distribution, pressure distribution, and velocity and the concentration of the gas must be measured all the time.

Thermocouples are installed on crucial positions of the reactor, to monitor and evaluate the temperature distribution during the experiments. Thermocouple bushings are distributed all over the reactor. (Figure 3.14)

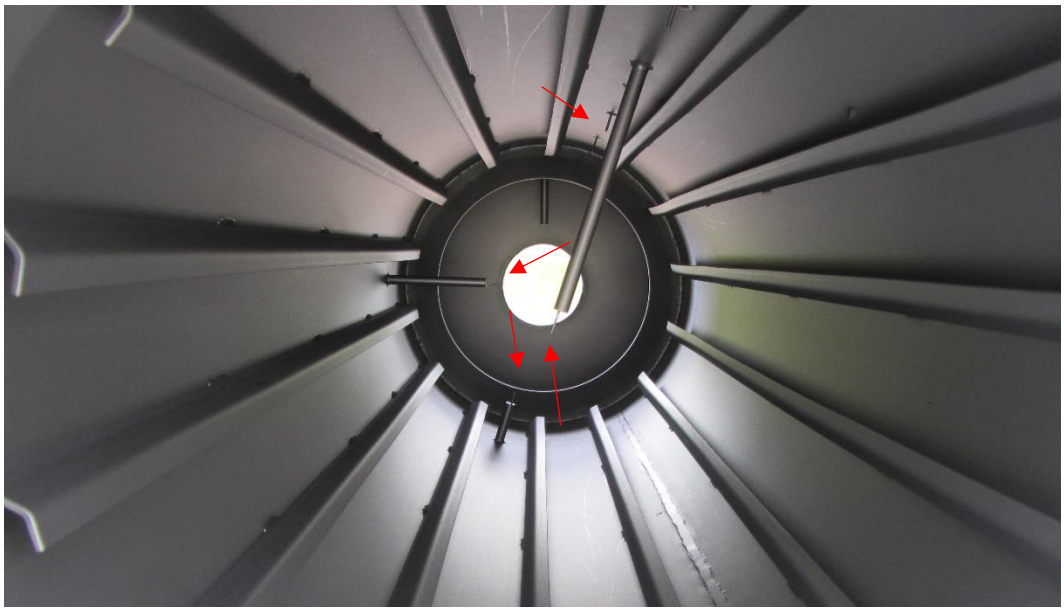

Figure 3.14 The inside of the reactor (arrows pointing at thermocouples)

These are then connected to a WLAN-module, which is fixed onto the frame of the cylinder. The NI-Module (Figure 3.15) registers the data, during the experiments, and sends the data to a corresponding receiver through a wireless connection, where the data can be studied and evaluated.

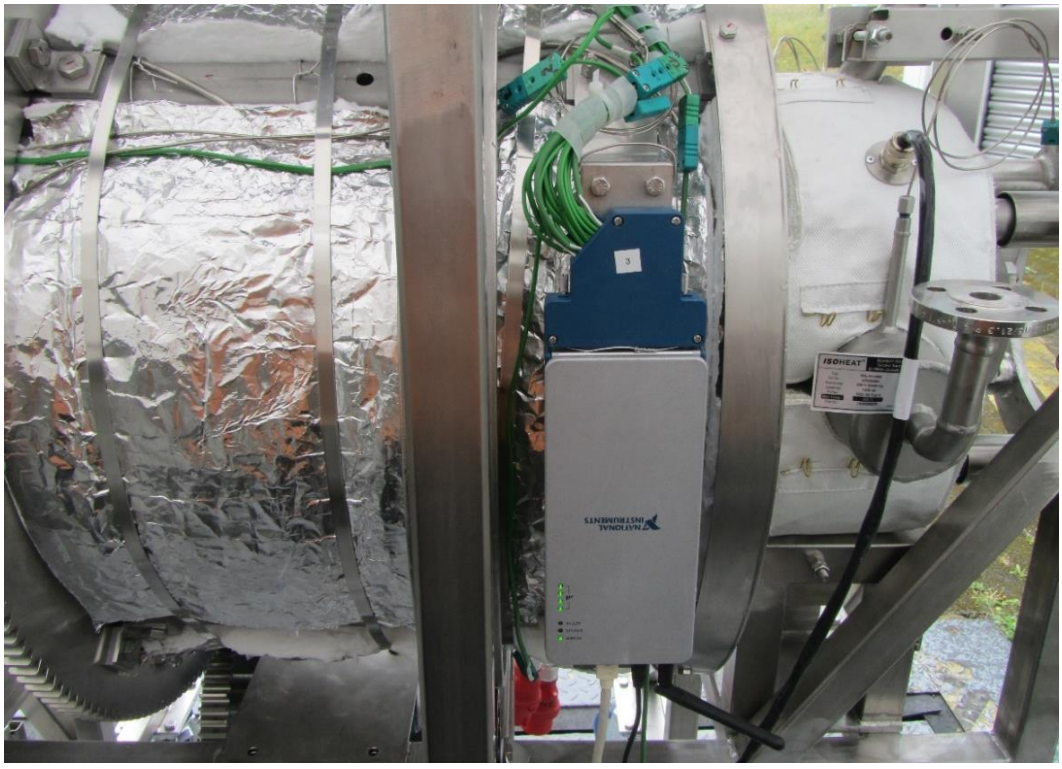

Figure 3.15 Thermocouples connected to the NI-Module

The pressure sensor is also fixed onto a bushing, however not on the cylinder itself but on the gas outlet-side and then directly connected to the control cabinet.
The most crucial task is the detection of the CO_2 concentration inside the system since it is an indicator of the efficiency of the reaction. Due to issues with the CO_2-sensor from the company Angst&Pfister, which will be explained more precisely later, a Micro Gas Chromatograph (GC) (490 Micro GC) was used as a quick and accurate alternative. The Micro GC is fixed onto the outlet of the filter unit. A small amount of gas will be sucked through a pipe, while the rest continues to flow through the system and is emitted into the environment. The gas flows through a mass flowmeter, which monitors the velocity of the gas at the outlet of the system, to check for lacks in the set-up. The flowmeter is also connected to the control cabinet.

g) Control cabinet

All the above mentioned elements, need to be controlled, regulated, and monitored. Doing this for each component and with different applications, would make the whole process to complicated and constraining. Thus, a general control device is needed, which regulates all the devices externally. A control cabinet links all the elements with their matching connection. This is the basis to create a device to control the whole system while using only one interface. An application such as Labview can be used, to create an interface between all the elements, to demonstrate the whole system, and to regulate it. (Figure 3.16)

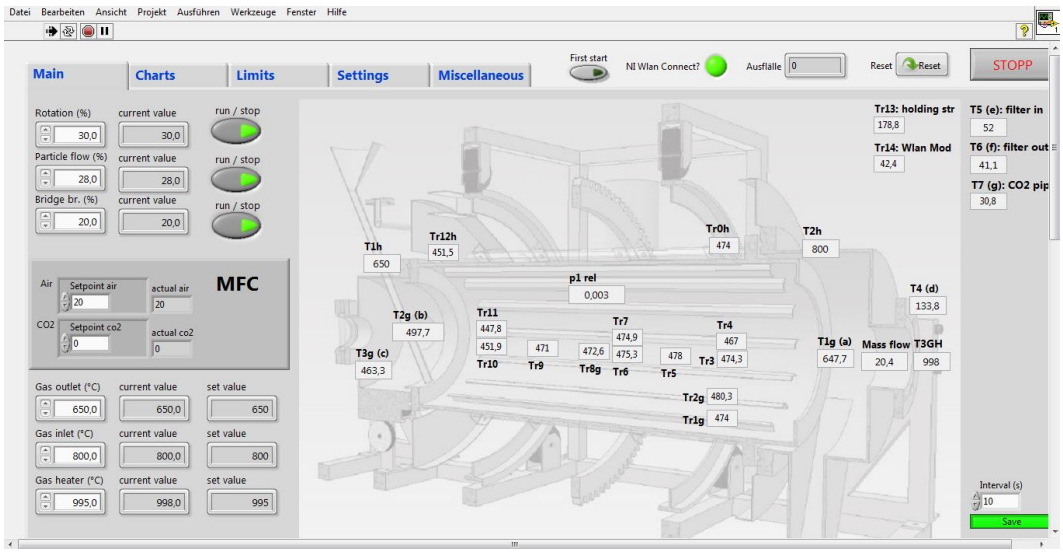

Figure 3.16 Labview interface for carbonator

The measured data can be saved to evaluate the process and its efficiency. The parameters, which will be monitored and regulated by the control cabinet, can be seen in the Table 3.1.

Table 3.1 Components and their parameters

Component	Corresponding parameter	Parameters to be set
Carbonator	rotational velocity (rpm)	frequency of Motor (Hz)
Screw feeder (feeding unit)	mass flow (kg/h)	frequency of Motor (Hz)
Screw feeder (bridge breaker)	rotational velocity (rpm)	frequency of Motor (Hz)
Heating components	temperature (°C)	temperature (°C)
Gas heater	temperature (°C) & velocity of gas (l/min)	temperature (°C) & velocity of gas (l/min)
Mass flow controller	velocity of gas (l/min)	velocity of gas (l/min)

4 Grain scale study

Before being able to conduct tests on lab-scale, a basic knowledge about the chemical balance of the reaction and the materials characteristics is required. The material which will be used during the whole experiments, was investigated in the Thermogravimetric Analyzer (TGA), to observe the reaction at different conditions and the reaction rate of the material. The TGA is an analytical method that records the change of mass of a sample exposed to a controlled temperature profile against the temperature. As already known, the TGA operates at ideal circumstances. It is a gastight system, with a constant heat and gas supply with a small-scale sample, which will be exposed to the heat and gas from almost all sides. For this reason, upscaling does not necessarily provide the same results. Nevertheless, the results provided from the TGA give a guideline value.

The following TGA (Figure 4.1) was conducted on CaO, which comes from the company NRW. An alternating carbonation and calcination were performed on the material. The Y-axis on the left shows the mass change in percent, and on the right side the temperature distributions in °C in red and the gas flow in ml/min in green. The X-axis shows the change of mass over time. The mass change symbolizes, that a reaction, of CaO binding CO_2 and forming $CaCO_3$, is taking place. The conversion rate can be calculated afterwards. The CO_2 concentration for the carbonation was 30 %.

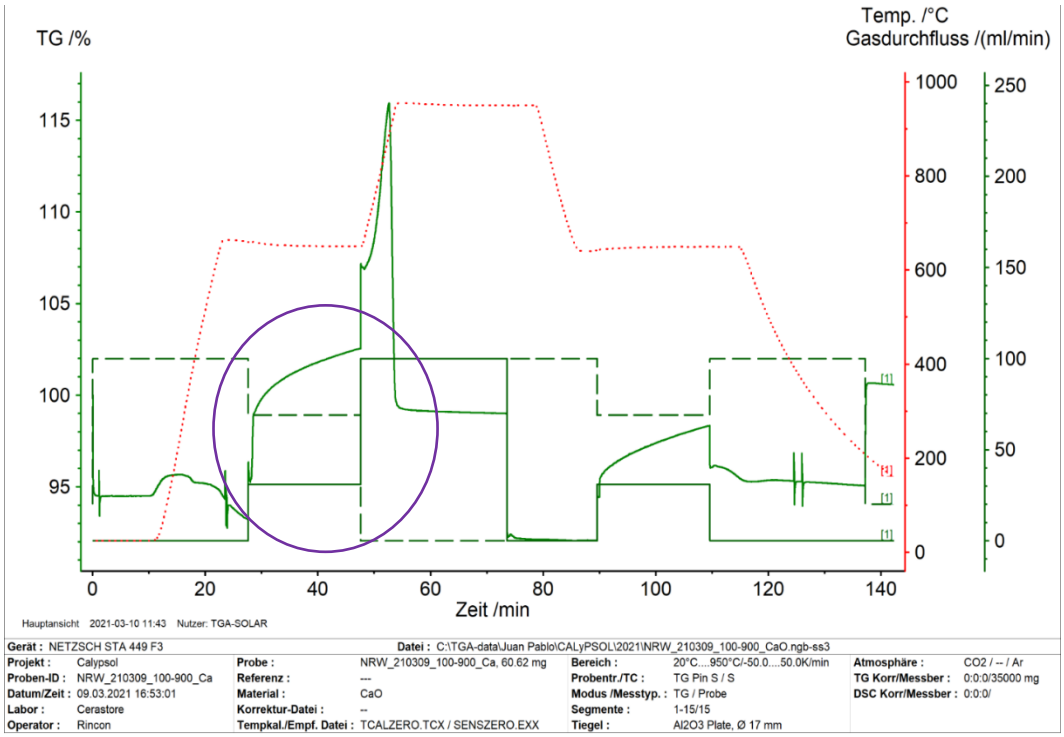

Figure 4.1 TGA on CaO conducting calcium looping

Based on this TGA outcome (Figure 4.1), the theoretically mentioned fast and slow carbonation stage in the earlier chapter is confirmed. Once the temperature inside the furnace reaches the carbonation temperature (650 °C), the weight of the material increases rapidly within approximately 1 min around 6 %. After that, the weight of the material increases only 3 % more within 19 min. This can be seen in the part, which is circled in purple. A minimum of 15 – 20 min is required, for the whole carbonation of the particles to take place, or at least, most of the carbonation. It follows that a minimum of one minute is at least required, for the reaction to start and after 2 min, 50 % of the carbonation takes place. This information is crucial since a minimum time can be defined for the particles to remain inside the furnace and to aim a complete reaction. The residence time which is a key parameter for the carbonation along to the temperature distribution, the materials reactivity, and the concentration of CO_2 inside the gas mixture. At this stage, to be able to set the operation conditions for the system, an understanding of the CaL reaction is first required.

The measure of the numerical relationship of the products and reactants is known as the stoichiometry. Based on the chemical reaction of the materials, initial conditions can be set.

The carbonation reaction equation:

$$CaO + CO_2 = CaCO_3 \quad (1)$$

with the following molar mass:

$$M(Ca): 40.078 \frac{g}{mol}$$

$$M(O): 15.999 \frac{g}{mol}$$

$$M(C): 12.011 \frac{g}{mol}$$

results to:

$$M(CaCO_3): 100.08 \frac{g}{mol}$$

with a substance ratio of 1:1.

In order to understand the whole reaction better, some initial conditions will be given to serve as an example. The initial values are 5 kg/h of CaO flow aiming to determine the corresponding volume flow for a conversion rate of 100 %. The concentration of CO_2 is 20 %. The calculation of the equation can be found in detail in the Appendix.

Based on the stochiometric balance, a volume flow of around 914 l/min is required, to fully react with the CaO and create $CaCO_3$. However, this is ideal stochiometric balance, where all the CaO is reacting with the CO_2, leading to a conversion rate of 100 %. There are some factors which need to be considered, while specifying the initial conditions for the experimental campaign, such as the residence time of particles and gas, the geometry of the furnace, and the real conversion rate of the material used. The overall goal of this project is to proof the carbonation with the carbonator and to maximize the CO_2 capture efficiency rather than reaching a high conversion rate of the particles, since the overall study is about the potential of carbon capture possibilities and new innovative ideas to reach this.

Having a look on the geometry of the reactor, with the diameter of 350 mm and a total length of 857 mm, the volume of the reactor is around 83 l. For a gas flow of around 914 l/min at 20 °C corresponding to 15 l/s at 700 °C, the contact time between the gas and the particles would be around 5 s for a mass flow of 5 kg/h based on the stoichiometric balance. Since one minute is at least required for the reaction to start and 2 min for 50 % of the carbonation to take place, the before calculated volume flow of 914 l/min is not suitable. For this reason, other aspects need to be considered, while determining the volume flow of the gas mixture.

A higher volume flow would favor the reaction and the conversion rate of the material used, however with the geometry of the reactor, the required residence time wouldn't be reached and thus the reaction might not take place at all. A lower flow would favor the capture efficiency of the system. However, the conversion rate of the material would decrease, and the full potential of the material wouldn't be used. A compromise between these two must be made. Taking all the mentioned factors in account, choosing a gas flow below the one resulting from the stochiometric balance (914 l/min), is required to reach the desired residence time, and to favor the capture efficiency of the whole system. The gas flow of 31 l/min with an initial CO_2 concentration of 20 % remains slightly more than 2 minutes inside the reactor, namely 2.7 minutes. We considered that this time should be enough, to start the reaction and extract most of the CO_2 out of the flue gas. During all these experiments, the gas flow of 31 l/min will remain the same, while the concentration of the CO_2 will be modified to see the impact of CO_2 change.

All in all, conditions for the further course were investigated throughout the analysis of the TGA results. One of the two main exclusions determines the minimum time required for the particles to remain inside the furnace to fully react, namely at least 15 minutes. For this reason, a residence time of average 20 minutes is targeted throughout the whole process. Another striking point is the volume flow of 31 l/min of the gas mixture, and which will be set as the standard flow all throughout the experimental campaign.

5 Cold tests

There are crucial parameters, which affect the outcome of the tests. These are the temperature distribution inside the furnace, the residence time of the particles, the mass flow of the fresh particles, and the volume flow of the gas mixture, which can be adjusted to favor the efficiency of the CaL process. Before aiming for the chemical reaction, some preparations needed to be done, for the system to be running. While some major components needed to be calibrated, to have a range of potential values to vary during the tests, doing tests on the carbonator in the cold state (ambient temperature) can be beneficial to save time. Simple tests such as observing the behavior of the particles inside the reactor can be done in the cold state, without wasting time on heating up the whole system for hours.

5.1 Rotational velocity of reactor

Figure 5.1 Mounted carbonator

The carbonator is rotating around its own axis set in motion by the motor. Particles coming from the screw feeder, will glide into the rotary cylinder and will be in a forward motion due to the rotation of the reactor.

These particles remain in the reactor for a certain time, named as the residence time. The residence time is a key factor during the whole test series and depends strongly on the rotational velocity of the reactor, the mass flow of the material, and on the angle in which the reactor is tilt. For this reason, the rotational velocity of the reactor must be studied to choose the best value and improved operations. Hence, the variables for the rotation of the reactor must be defined through setting the motor which will transmit the motion onto the reactor. The motor is connected to a frequency convertor with a range of 0 – 50 Hz. Once a particular frequency is set, the time will be measured for the reactor to turn around. This will be repeated for different frequencies, and results are plotted in the diagram in Figure 5.2. From these experimental results, a linear correlation can be made, and will be used as the reference for the further procedure.

Table 5.1 Experimental investigation of time needed for one full rotation of the reactor

Frequency in Hz	**Duration of a full rotation in s**					**Mean value in s**
	1.	2.	3.	4.	5.	
20	51.82	52.8	50.51	52.17	51.95	51.85

Table 5.2 Frequencies and their corresponding values for rotational velocity

Frequency in Hz	**Mean value from measurements in s**	**Rotational velocity in 1/min**
5	210.00	0.29
10	104.00	0.58
15	68.67	0.87
20	51.85	1.16
25	41.31	1.45
30	34.40	1.74
35	29.58	2.03
40	25.77	2.33
45	22.92	2.62
50	20.69	2.90

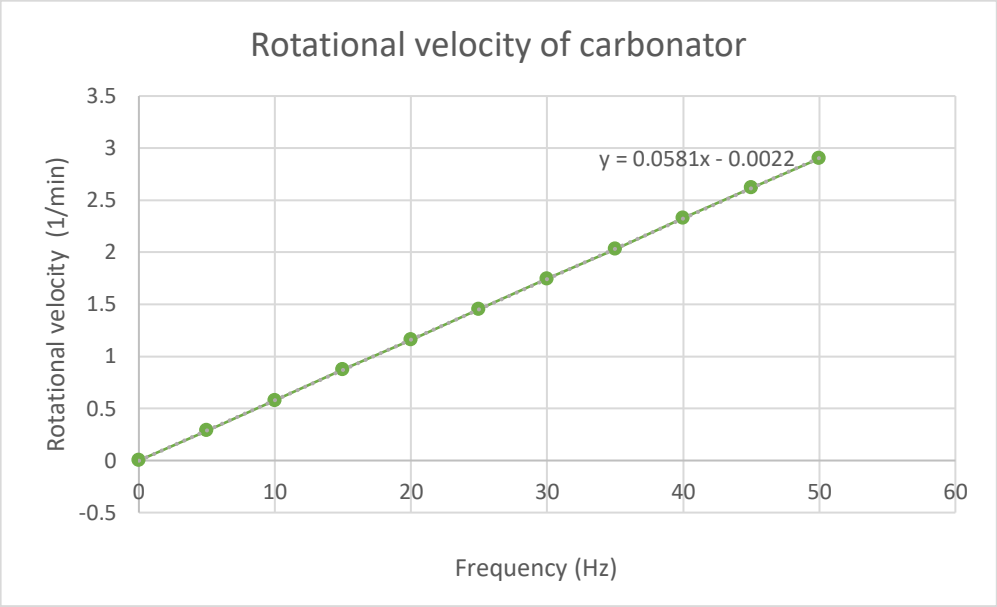

Figure 5.2 Rotational velocity of carbonator as a function of frequency

Based on the outcome of the tests, the rotational velocity behaves linear to the frequency, thus the equation (2) can be used to determine any required velocity.

$$y = 0.0581x - 0.0022 \quad (2)$$

From our experimental tests, the rotational velocity ranges between 0.29 – 2.90 rpm.

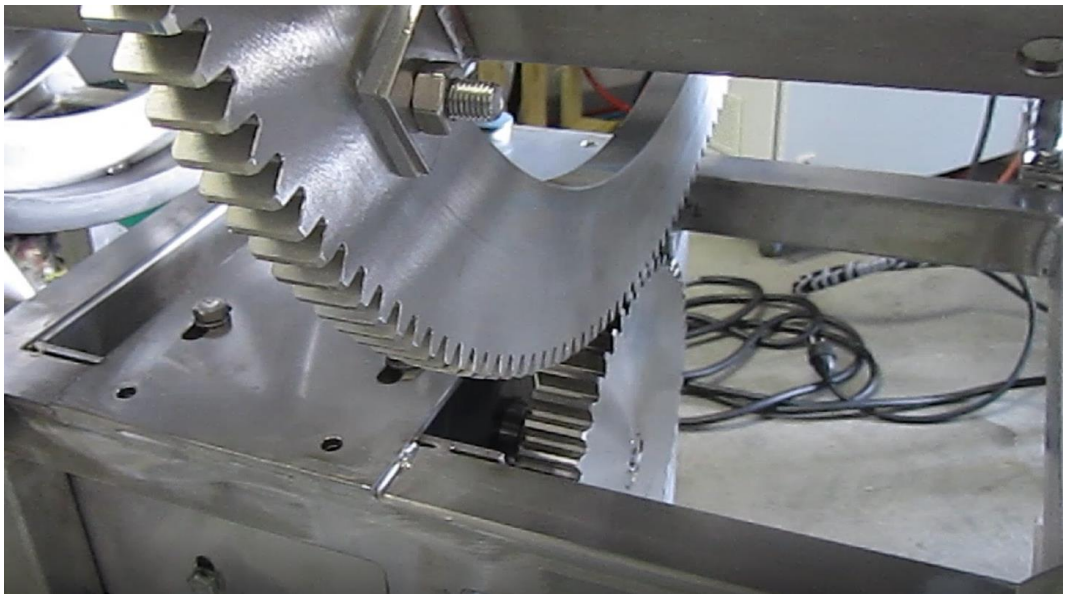

Figure 5.3 The two intermeshing gears

5.2 Screw feeder

The screw feeder enables the particle feeding during the experiments. The rotational velocity of the screw determines the mass flow of the particles. Since the mass flow is one key parameter, which will be modified during the tests with the flue gas, it is important to know in which manner the particles move. Due to the size, the density, the weight, and other properties of the used materials, the screw feeder must be calibrated for each material used during the experiments. In this case, the screw feeder must be calibrated for the material CaO from the company NRW.

The screw of the feeder rotates around its own axis, driven by a motor, regulated through a frequency converter. Its range reaches from 0 – 50 Hz.

In order to estimate the mass flow of the particles, the mass of the falling particles have to be weight for a certain period of time, usually one hour. This must be done for different frequencies, in order to create a relation between the frequency and the mass flow.

5.3 Test series: Calcium oxide (CaO)

During the calibration of the screw feeder with the material CaO, some difficulties occurred. During the first test, it was observed that after starting the screw feeder, the particles stopped falling shortly after. We noticed that the exit of the screw feeder was blocked, and the particles became denser, while the screw feeder was running. Aiming to find the cause of this matter, the particles were examined with a sieve shaker and the results are summarized in Table 5.3 and Figure 5.4.

Table 5.3 Distribution of particle size after going through sieve shaker

		< 100µm		100 < X < 300µm		300 < X < 500µm		500 < X < 700µm		700 < X < 900µm		> 900µm		Total	Sum	Mass
Date	Test	Mass [g]	Mass[%]	Mass [g]	Mass[%]	Mass [g]	Mass[%]	Mass [g]	Mass[%]	Mass [g]	Mass[%]	Mass [g]	Mass[%]	Mass [g]	Mass[g]	[%]
15.04.2021	1	45.12	20.51	65.75	29.89	10.31	4.69	7.64	3.47	6.77	3.08	84.14	38.24	220.01	219.73	99.87
	2	45.59	20.72	65.38	29.72	10.97	4.99	7.63	3.47	6.84	3.11	83.38	37.90	220.02	219.79	99.90
	3	44.65	20.29	64.61	29.36	11.65	5.29	7.58	3.44	7.40	3.36	84.06	38.20	220.04	219.95	99.96
	4	43.20	19.64	66.71	30.32	11.66	5.30	7.80	3.55	6.98	3.17	83.32	37.87	220.00	219.67	99.85
	5	41.69	18.95	62.23	28.28	16.52	7.51	7.94	3.61	7.07	3.21	84.39	38.35	220.04	219.84	99.91
	mean	44.05	20.0207	64.936	29.5135	12.222	5.55486	7.718	3.50783	7.012	3.18695	83.858	38.1135			

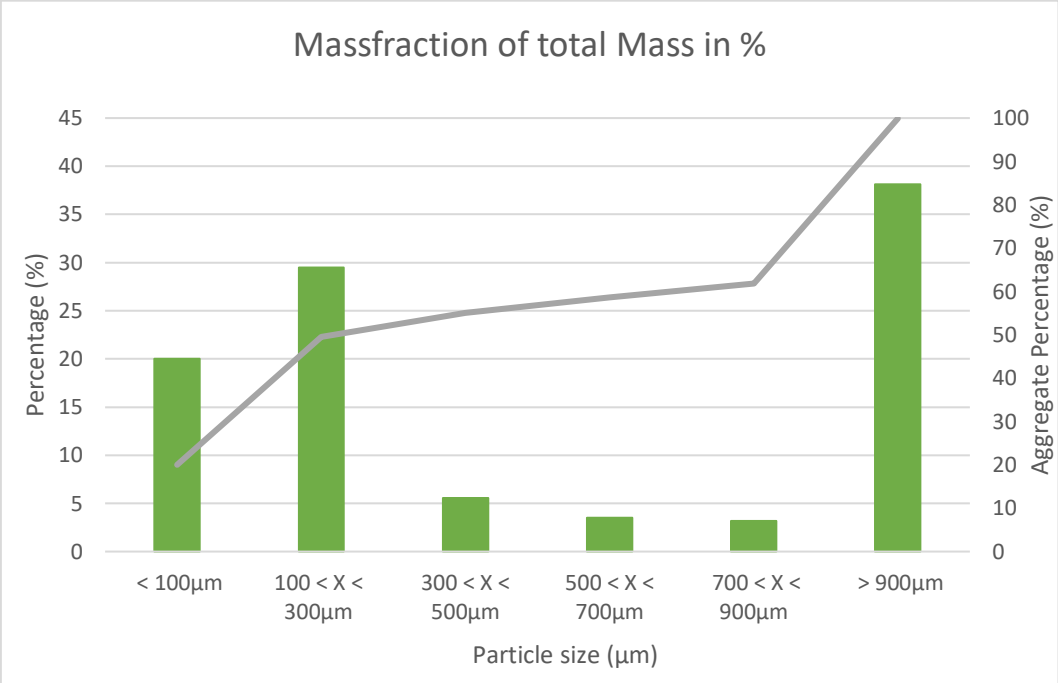

Figure 5.4 Test with sieve shaker: Distribution of particle size of used CaO in %

It is clearly visible, that more than 50 % of the total mass of the particles are distributed between < 100 µm and 300 µm. Particles in this size range tend to agglomerate to each other and won't glide down as expected. The fine particles stick to each other and create a bridge above the screw, blocking the rest of the particles. Also, it is commonly known that CaO tends to absorb moisture out of the air as it reacts to calcium hydroxide. Cause the CaO remains in the screw feeder open to the experimental room, it absorbs the water of the surrounding air, making the particles stickier and harder to handle.

After observing this phenomenon, we decided to use a bridge breaker. (Figure 5.5) It breaks the constantly forming bridge of particles and guarantees a permanent flow of particles.

Figure 5.5 Inside of the screw feeder (bridge breaker)

The following Table 5.4 serves as an example of a typical calibration to estimate each mass flow for a corresponding frequency. In this case the frequency was set to 20 Hz and the mass of the falling particles was measured in a certain time interval. The idea in determining the mass flow is to compare the actual weight at the end of the calibration compared to the predicted one.

Table 5.4 Determined mass flow of CaO for one hour test period for the frequency 20 (Hz)

Time (min)	Mass (kg)	Difference	Determined Mass flow (kg/h)
0	0	0	0
5	0.965	0.965	11.58
10	1.945	0.98	11.76
15	2.925	0.98	11.76
20	3.89	0.965	11.58
25	4.85	0.96	11.52
30	5.79	0.94	11.28
40	7.57	1.78	10.68
50	9.26	1.69	10.14
1 hour = 60	10.475	1.215	7.29
			∅ 10.84

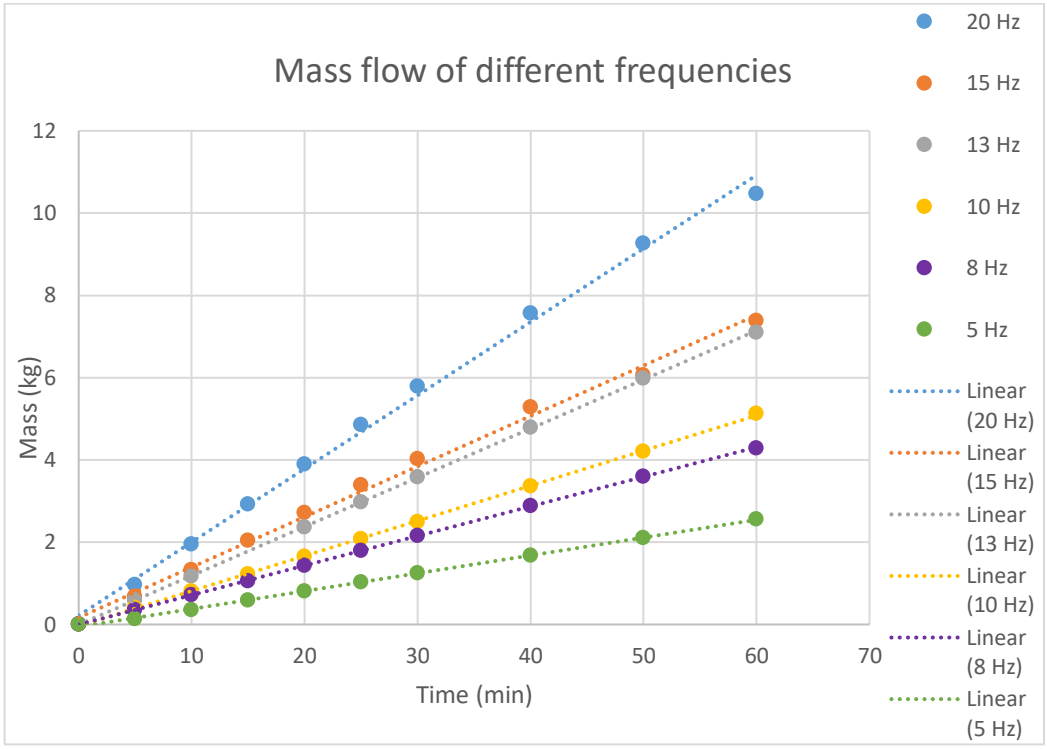

Figure 5.6 Determined mass over time for different frequencies

As seen in Figure 5.6, the mass flow of CaO is not ideally linear for none of the frequencies. This is because the particles aren't flowing uniformly, due to their size and the tendency to agglomerate to each other. The measured mass after one hour doesn't fit with the determined mass flow of the corresponding frequency visible in Table 5.5.

Table 5.5 Mass flow corresponding to different frequencies (Hz)

Frequency (Hz)	Mass flow after 60 min (kg/h)	Determined Mass flow (kg/h)
5	2.560	2.537
8	4.290	4.300
10	5.130	5.080
13	7.105	6.848
15	7.385	7.610
20	10.475	10.843

However, having a look on the Figure 5.7 it is clearly visible, that the deviation from the predicted mass flow is minimal, if not almost invisible. The support of the bridge breaker ensures an approached linearity.

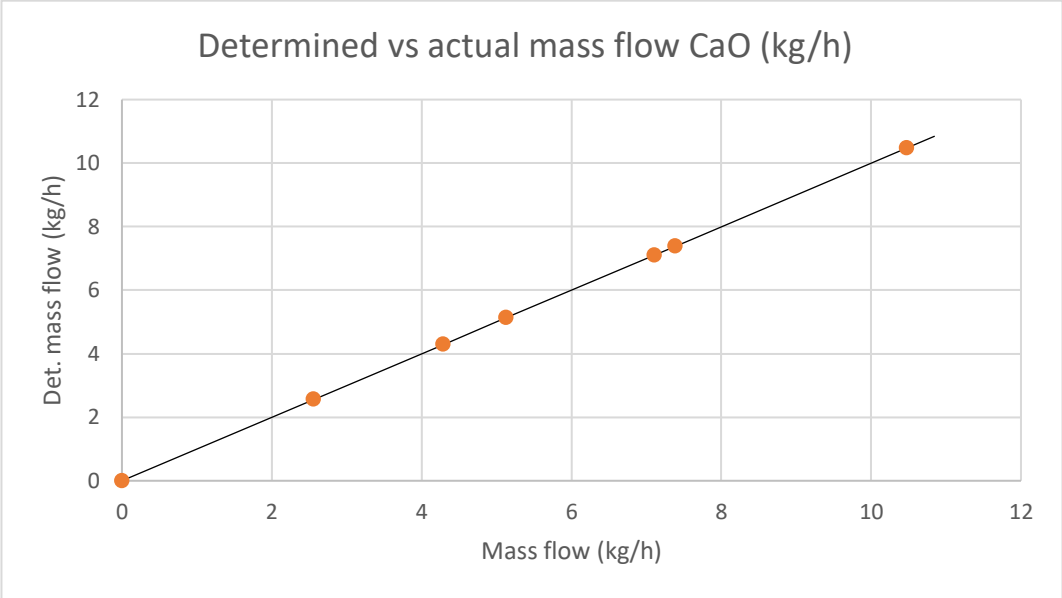

Figure 5.7 Determined mass flow over actual mass flow (kg/h)

5.4 Residence time

The residence time can be defined in various ways, based on the field of application. In this current case, residence time can be understood as the time of a particle first entering the reactor until it exists the reactor. It is the timespan where the material can react with the CO_2 of the flue gas.

Based on the TGA results, which were generated to study the behavior of the material, all the calcium oxide reacts within 20 minutes. 80 – 90 % of the reaction takes place within a short time after getting in contact with the gas, while the remaining conversion lasts around 15 minutes. In addition to the residence time, the distribution of the particles inside the reactor is a key point for the reaction rate.

If the particles are uniformly distributed inside the reactor, all the particles get in contact with the flowing flue gas, which will improve the reaction rate.

The residence time starts once the first particle falls inside the reactor and stops once the same particle will fall into the storage. However, the time measured is only an approximation since the movement of the particles inside the reactor is hard to determine, while observing the whole movement through the window on the particle entrance side.

Since calcium oxide can be hazardous, it is important to avoid releasing it into the surroundings while handling it. Therefore, the reactor must be closed. It is possible to observe the process through the window.

This however may cause difficulties since the particles are fine and start to create dust inside the reactor.

The residence time depends on three parameters, the rotational velocity of the reactor, the mass flow of fresh particles inside the reactor, and the angle of tilt of the reactor. During the calibration, one parameter was modified, while the others were kept constant, and this was done for each parameter respectively. Results are summarized in the following tables and figures. (Table 5.6, Table 5.7, Table 5.8, Figure 5.8, Figure 5.9, Figure 5.10)

Table 5.6 Vatiation of the mass flow of particles

Mass flow screwfeeder in kg/h	**Observation**	**Angle in °**	**Rotational velocity in rpm**	**Residence time in min**
approx. 10,84 kg/h = 20 Hz	well distributed in room	6°	15Hz = 0.87 rpm	15:52
approx. 7.385 kg/h = 15 Hz	particle falling evenly	6°	15Hz = 0.87 rpm	17:35
approx. 6.85 kg/h = 13 Hz	particle falling evenly	6°	15Hz = 0.87 rpm	20:22
approx. 5.13 kg/h = 10 Hz	particle falling evenly	6°	15Hz = 0.87 rpm	21:14
approx. 2.56 kg/h = 5 Hz	falling slowly, not distributed in room	6°	15Hz = 0.87 rpm	30:35

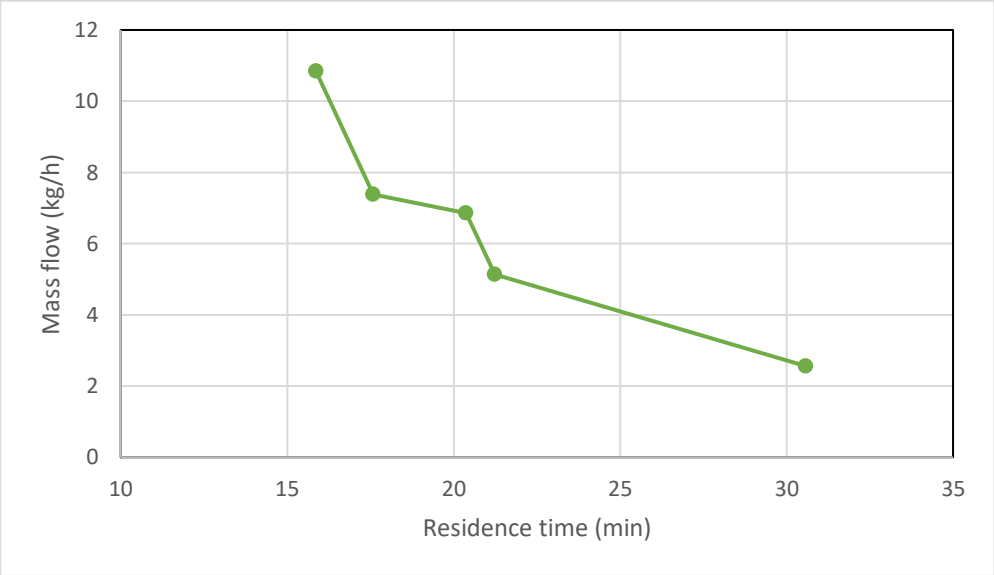

Figure 5.8 Mass flow over residence time

Table 5.7 Variation of reactors tilting angle

Angle in °	**Observation**	**Mass flow screwfeeder in kg/h**	**Rotational velocity in rpm**	**Residence time in min**
5°	particle falling evenly, well distributed in room	approx. 7.385 kg/h = 15 Hz	20 Hz = 1.16 rpm	17:53
6°	particle falling evenly, well distributed in room	approx. 7.385 kg/h = 15 Hz	20 Hz = 1.16 rpm	15:25
7°	particle falling evenly, well distributed in room	approx. 7.385 kg/h = 15 Hz	20 Hz = 1.16 rpm	13:48
8°	particle falling evenly, well distributed in room	approx. 7.385 kg/h = 15 Hz	20 Hz = 1.16 rpm	12:24

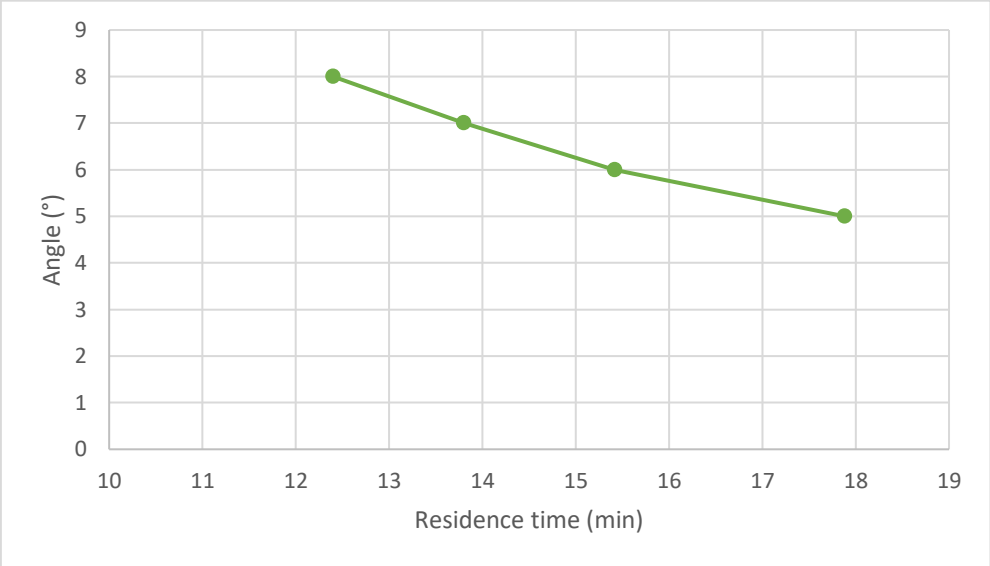

Figure 5.9 Angle of tilt over residence time

Table 5.8 Variation of the rotational velocity of the reactor

Rotational velocity in rpm	**Observation**	**Mass flow screwfeeder in kg/h**	**Angle in °**	**Residence time in min**
10 Hz = 0.58 rpm	particle falling slow and evenly, well distributed in room	approx. 7.385 kg/h = 15 Hz	6°	16:50
15 Hz = 0.87 rpm	particle falling evenly, well distributed in room	approx. 7.385 kg/h = 15 Hz	6°	17:35
17.2 Hz = 1 rpm	particle falling evenly, well distributed in room	approx. 7.385 kg/h = 15 Hz	6°	16:11
20 Hz = 1.16 rpm	particle falling evenly, well distributed in room	approx. 7.385 kg/h = 15 Hz	6°	15:25
25 Hz = 1.45 rpm	particle falling evenly, well distributed in room	approx. 7.385 kg/h = 15 Hz	6°	12:06
34.4 Hz = 2 rpm	particle falling evenly, well distributed in room	approx. 7.385 kg/h = 15 Hz	6°	08:21

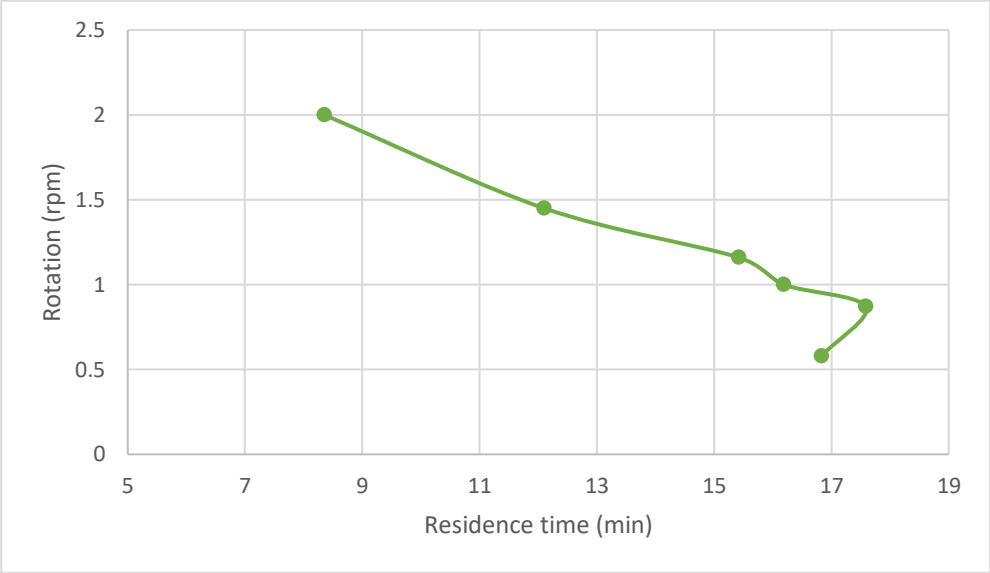

Figure 5.10 Rotation of reactor over residence time

During all the tests, the movement of the particles were observed, since the distribution inside the reactor is also a key factor to determine the ideal conditions. The angle of the reactor seemed to be ideal at 6°, because the particles are falling evenly and spread all over the reactor. For this reason, keeping the angle at 6° for the following hot tests and chemical tests, is a good initial assumption.

Based on the conducted tests, the variables can be modified to reach the desired residence time. Since the results are only based on rough estimations, it is important to change the conditions around the designated variables, to achieve the highest efficiency during the experiments including the chemical reaction. According to the results of the tests, the angle of the reactor should be set to 6°, while the rotational velocity and the mass flow of particles can be adjusted, to roughly attain the residence time of 15 - 20 minutes.

Based on the cold tests, which were made to figure out the ideal conditions for operation regarding the residence time, the mass flow of approximate 7.8 kg/h, the rotation of 0.87 rpm, and the angle of 6° can be set, to achieve the desired residence time of the particles and ensure a uniform flow of the particles inside the reactor.

5.5 CO_2-sensor

To measure the efficiency of the system, a CO_2-sensor is needed. In our case, the CO_2-sensor measures concentrations between 0 – 30 % CO_2 for a volume flow between 0 – 150 l/min of the gas mixture. Usually, these gas mixtures consist of CO_2, N_2, H_2O, and O_2. For the experiment, this can be roughly imitated by mixing a pure stream of CO_2 and pressurized air. The concentration of CO_2 can then be varied by fixing the volume flow of the pure stream and the pressurized air.

A CO_2-sensor from the company Angst & Pfister was intended to use for the experiments. The sensor measures three points per second. The calibration of the sensor for the same range as the experiments was successful, however the measurements during the first experiments were not correct. For this reason, we switched, using the Micro GC. The GC is widely used as an analytical method for separating mixtures into individual chemical compounds. The substance to be analyzed is injected into a carrier gas (argon, nitrogen, helium), which then flows through a separation column. The separation column contains a porous test substance as the stationary phase. As a result of the distribution equilibrium between the stationary phase and the gas phase, which is characteristic for each substance, the individual components reach a detector at different times. Since the retention time (time between injection and detection of the components) is substance-specific, an indication of the type of substance present is obtained under constant conditions by comparison with reference substances. The GC, in contrast to the CO_2-sensor, gives out one point every three minutes. Therefore, a sudden change of the CO_2 concentration will not be visible, but an overall change and difference in the concentration over time can be observed.

The value in the GC will be given out as µV.min. The conversion to percent can be done using the following equation (3).

$$y = (x + 48.895)/349.21 \tag{3}$$

y equals the concentration in percent and x is the value given out from the GC in µV.min.

The GC was installed at the end of the system to measure the concentration of the gas, which went through the whole cycle. During the calibration, the concentration of CO_2 inside of the gas mixture was varied to see if the GC will respond in the same manner. The volume flow of the gas mixture needs to remain the same during the whole calibration, to have a valid result in the end. The airflow is set to 100 l/min.

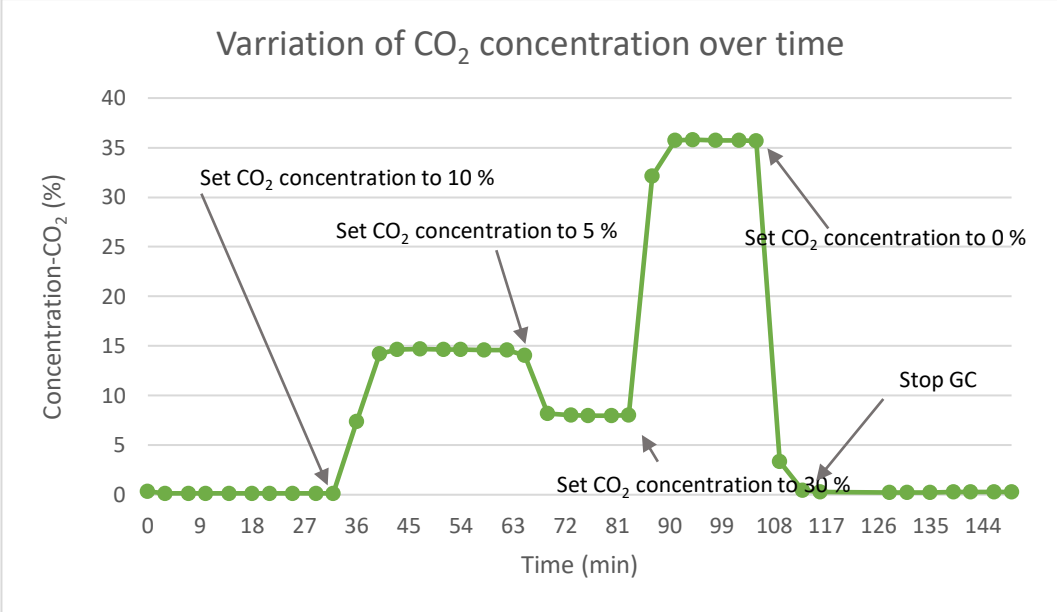

Figure 5.11 Varying CO_2 concentration over time measured in Micro GC

According to Figure 5.11 we can see that the GC is sensitive enough to answer to a change of the concentration. The calibration took place at the same state as the actual tests, so the calibration curve can be used to estimate the CO_2 concentration for the following chemical tests.

6 Hot tests

The carbonation inside the reactor takes only place when the temperature reaches more than 650 °C. All the heating elements which were installed all over the carbonator shall contribute to achieve the desired temperature inside the reactor. Up until now the system was tested in a cold state. However, since steel will expand with rising temperatures, there might be the risk, that the system will get too tight and forces exert on the bearing, eventually leading to wear and malfunction of the system. The Hot tests are carried out without any particle and gas flow to achieve the desired temperature, observe the heating reactor of the system, and to make sure that each of the used components will work together.

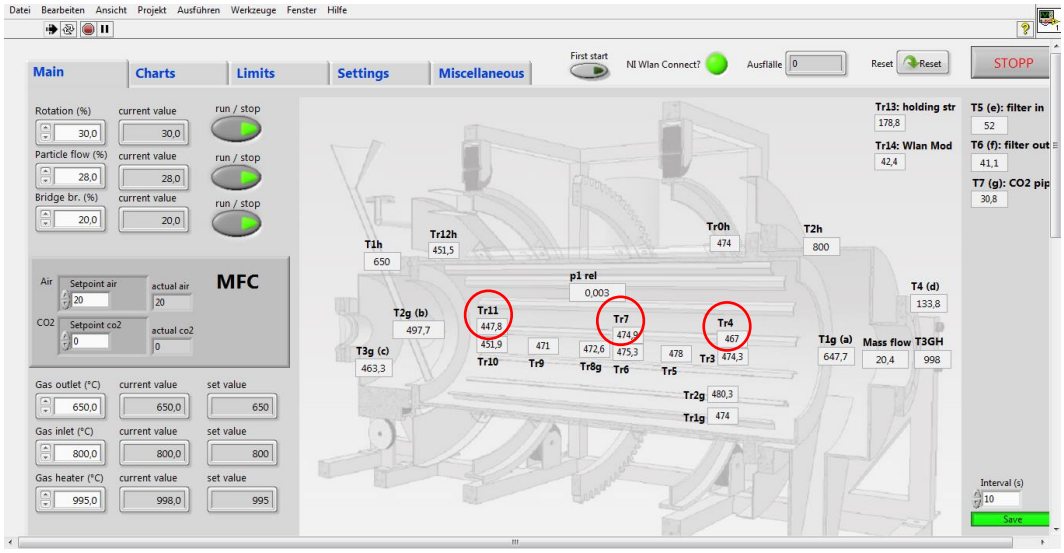

Figure 6.1 Labview interface for carbonator with instantaneous temperature specification

The aim was to reach at least 650 °C inside the reactor. Since steel is inert, the whole process of reaching the proper temperature could take a long time. The idea was to slowly increase the temperature of the system, step by step, until the temperature distribution for the whole system becomes stationary. This step was done to observe the heating behavior of the system. The heat input comes from the heating cable, which is wrapped around the cylinder of the reactor and plugged into the power supply of the room, the gas heater, and the heating sleeves at the gas-inlet and gas-outlet.

The temperature of all the heating elements were increased by 50 – 100 °C every 10 – 30 min once the temperature inside the reactor stabilized and reached the input value. Once all heating elements are set to their maximum temperature and a steady temperature distribution is reached all over the reactor, the heating cable can be unplugged. After unplugging the heating cable, the rotation of the carbonator and the injection of the particles can be started. This part is especially important, to observe the change of temperature once the heating cable doesn't contribute to the heating of the system anymore and the cold particles or "particles at ambient temperature" enter the carbonator.

Since all heating elements and the NI Module as well, are connected to the control cabinet, the data can be directly displayed through an interface created in LabVIEW. The data can be saved for further evaluations. The Figure 6.2 shows the first half of the hot tests, where the carbonator is first heated up. It visualizes the temperature distribution inside the carbonator.

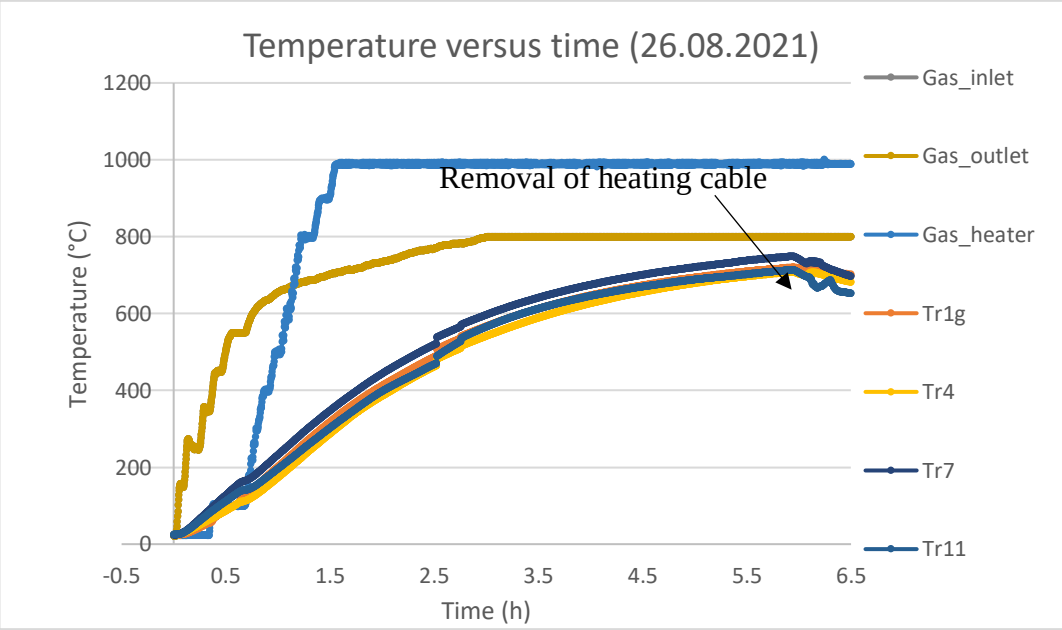

Figure 6.2 Temperature curves of heating elements and thermocouples over time without CO_2 input (26.08.21)

The curves Gas_inlet, Gas_outlet and Gas_heater represent the temperature curve of the heating elements used during these experiments, whereby the curves Gas_inlet and Gas_outlet, represent the temperature distribution of the heating sleeves.

Based on the data sheet, the heating sleeves can be heated up to maximally 1000 °C. But due to heat losses, the maximum temperature of 1000 °C cannot be reached. Thus within 5 hours the maximum of around 800 °C is reached (grey, dark yellow). Since the heating cable is connected externally, there is no data recorded for it, however the maximum temperature reached during the experiments was around 800 – 900 °C. The gas heater can reach the maximal temperature of 1000 °C (light blue), whereas the actual gas temperature (orange) is beneath the temperature, around 700 °C the highest. To fasten the heating process, the volume flow of the gas is set to a high value, around 100 l/min. The three lines at the bottom represent the overall temperature distribution inside the reactor, since they are measured at the front part (Tr 4), middle part (Tr7), and end part of the carbonator (Tr11). (Figure 6.1)

The temperature inside the carbonator rises steadily, while increasing the temperature of the heating elements constantly. Once the maximal temperature of the heating elements is reached, the temperature inside of the reactor increases moderately until it reaches an almost constant value. As seen in Figure 6.2 there is a temperature drop after around 6 hours of heating, which is due to the unplugging of the heating cable. This is however not too drastic, since the temperature is on an already high level and the temperature decreases gradually. Based on the recorded data, Tr4, Tr7, and Tr11 reach the highest temperature of 709 °C, 749 °C, and 714 °C respectively. This temperature should be ideal for the reaction to take place. For this reason, a reaction is expected once the particles meet the gas flow in the following chemical tests. The whole heating phase takes around 5 – 6 hours, until reaching a suitable temperature distribution inside the reactor and the temperature nearly doesn’t increase anymore.

As mentioned before, a temperature drop due to injection of ambient temperature particles is expected, this behavior was also studied, before continuing with the chemical tests, to predict temperature distribution inside the reactor and guarantee a sufficient temperature for the whole process. The Figure 6.3 visualizes the temperature distribution from the 26th of August with the particle flow.

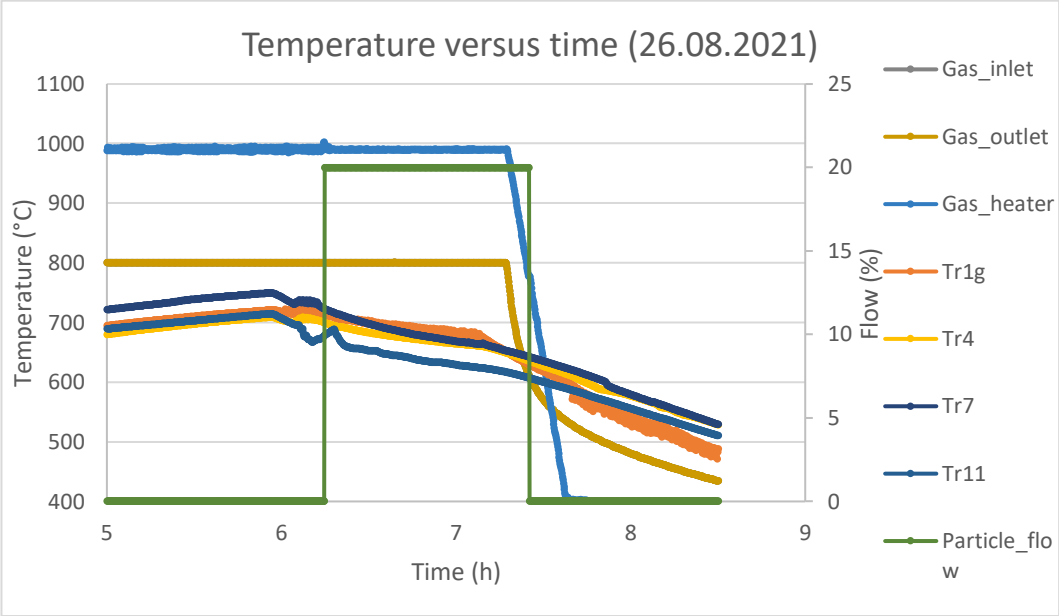

Figure 6.3 Temperature curves of heating elements and thermocouples and particle flow over time without CO_2 input (26.08.21)

The graph visualizes the second half of the heating phase, where particles get injected into the system. The Particle_flow curve (green) provides information about the particle flow inside the reactor. All in all, the injection of the particles lasted for around one hour. During that hour, the overall temperature of the system drops to around 80 °C. This can be drastic, if the temperature is below the carbonation temperature and the reaction can't take place anymore. For this reason, the temperature of the system must be high enough to compensate this loss of temperature and ensure a reaction. Counter measures will be evaluated and discussed in the following chapters.

Lastly, the cooling phase of the reactor must be considered as well. Indeed, the safety regulations specify a temperature inside the reactor, which shall be below 200 °C, before leaving it unsupervised. Another 2 – 3 hours after the particle injection phase are required until the reactor reaches that temperature.

Finally, after conducting a series of hot tests, it is crucial to consider the temperature drop, when unplugging the heating cable and injecting the particles. For this reason, the whole potential of the heating elements must be exploited during the heating phase. The heating phase for the following chemical tests will also take around 5 – 6 hours.

7 Chemical tests

Now that several essential tests were conducted and preparations were made, solid knowledge is available to start the experimental campaign of the chemical tests. The ideal conditions which were investigated during the cold and hot tests will be set as fixed parameters for the following chemical tests. Fixed variables are the rotational velocity and the angle of tilt of the reactor which lead to a residence time of 15 – 20 min, depending on the mass flow of the particles. Moreover, the temperature distribution inside the furnace and the volume flow of the gas mixture are also fixed. Variables which will be adjusted during the chemical tests are the CO_2 concentration inside the gas mixture and the mass flow of the CaO particles.

From the TGA, the residence time was chosen to be a fixed variable, intending to apply it for further experimental campaigns. However, there is a difference between the TGA, which represents an ideal system, and the reactor, which is a moving system. There might be the possibility, that the movement of the particles has a different effect on the carbonation reaction, and varying the residence time around a different range in contrast to the previously determined one, will lead to a better result. Due to lack of knowledge and time regarding this matter, it makes sense to continue with the assumption of the TGA first and modify parameters as mass flow of CaO and concentration of CO_2 to optimize the carbonation reaction and the efficiency of the system and start varying the "fix" variables afterwards.

During all of the experiments, the gas flow of 31 l/min will remain constant, whereby the concentration of CO_2 will be modified between 10 – 30 %, to analyze the impact of each CO_2 concentration on the reaction.

The efficiency of the system can be evaluated through the Micro GC and analyzing the particles which went through the reactor with the TGA.

As time was limited, a certain experimental plan was needed and is described in the Table 7.1.

From there, the mass flow will be varied between 5 – 7.8 kg/h. The concentration of CO_2 inside the flue gas flow will be varied between 10 – 30 % accordingly.

Table 7.1 Experimental plan during the chemical tests

	13th August	**20th August**	**26th August**	**27th August**	**31st August**	**6th September**	**8th September**	**10th September**
Particle mass flow (kg/h)	7.8	5	5	7.8	5	5	7.8	7.8
Desired Input CO_2 (%)	20	20	30	30	10	10	10	20
Actual Input CO_2 (%)	-	-	-	37	13	12	13	27
	With CO_2-sensor			With Micro GC				

Experimental conditions:

Reactor rotation: 0.87 rpm

Duration of reaction: 1 h (approx.)

Temperature before injecting particles: 700 °C < T < 750 °C

7.1 Experimental description

The experimental conditions as angle of inclination, rotation etc. have been defined from the previous cold tests campaign and will remain the same. The rotation will be controlled through Labview, and the temperature regulated through the control boxes and the interface in Labview. The procedure of the chemical tests is identical to the hot test, up to one point, where CO_2 shall be injected into the system. Just like during the hot tests, the temperature will be increased step by step. To fasten the heating process, the airflow of the gas heater is set to 100 l/min. Once the maximal temperature of the heating elements is reached, and the temperature inside the reactor stabilized, the particle injection can be started. Before injecting the particles, the airflow must be adjusted. The total airflow is reduced from 100 l/min to 31 l/min with the desired CO_2 concentration. Simultaneously, the Micro GC will be started. Once, the desired temperature is reached, and the CO_2 concentration stabilizes, the particle injection can start.

Usually, the injection phase of particles takes up to one hour, to ensure the same condition for each test run. Since the heating phase usually takes around 5 – 6 hours, and the cooling phase also takes around 2 – 3 hours, the injection phase is reduced to 1 hour.

The following Table 7.2 specifies the conditions, which were applied for the test of the 8th of September.

Test: 10 % of CO_2 – 7.8 kg/h of CaO

Table 7.2 Set parameters for experiment with 10% CO_2 and a particle flow of 7.8 kg/h

Variable	Variables	Set value
	CO_2 concentration (%)	10 %
	CaO flow (kg/h)	5 kg/h
Fixed	Temperature (°C)	600 – 700 °C
	Rotation reactor (rpm)	0.87 rpm
	Angle of tilt (°)	6 °

The Figure 7.1 visualizes the recorded temperature inside the reactor, during the whole experiment.

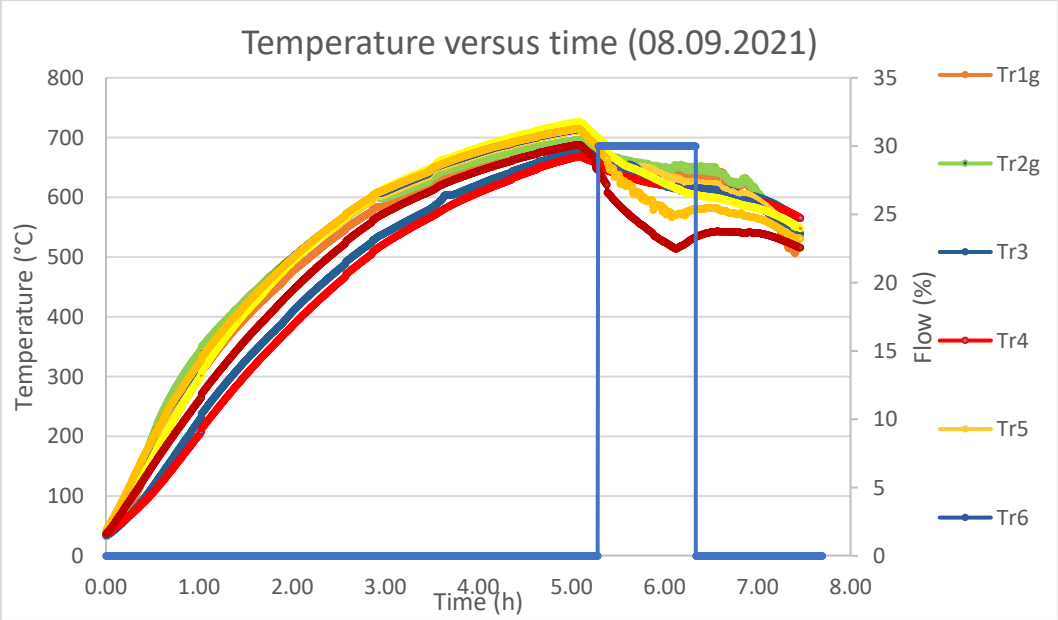

Figure 7.1 Temperature curves of thermocouples and particle flow over time with 10% CO_2 input (08.09.2021)

The different curves in the Figure 7.1 show the temperature distribution inside the reactor measured by the single thermocouples (Tr1g, Tr2g, Tr3, Tr4, Tr5, Tr6, Tr7, Tr8, Tr9, Tr11). After 5 hours, the particles get injected and it is clearly visible, that the temperature of the system drops drastically once the particles enter the system. At the same time the Micro GC records data, which give information about the CO_2 concentration inside the reactor. A change of the CO_2 concentration symbolizes, that the carbonation reaction took place. The following Figure 7.2 displays the CO_2 concentration over time for the experiment of the 8th of September, with an initial CO_2 concentration of 10 % and a particle flow of 7.8 kg/h.

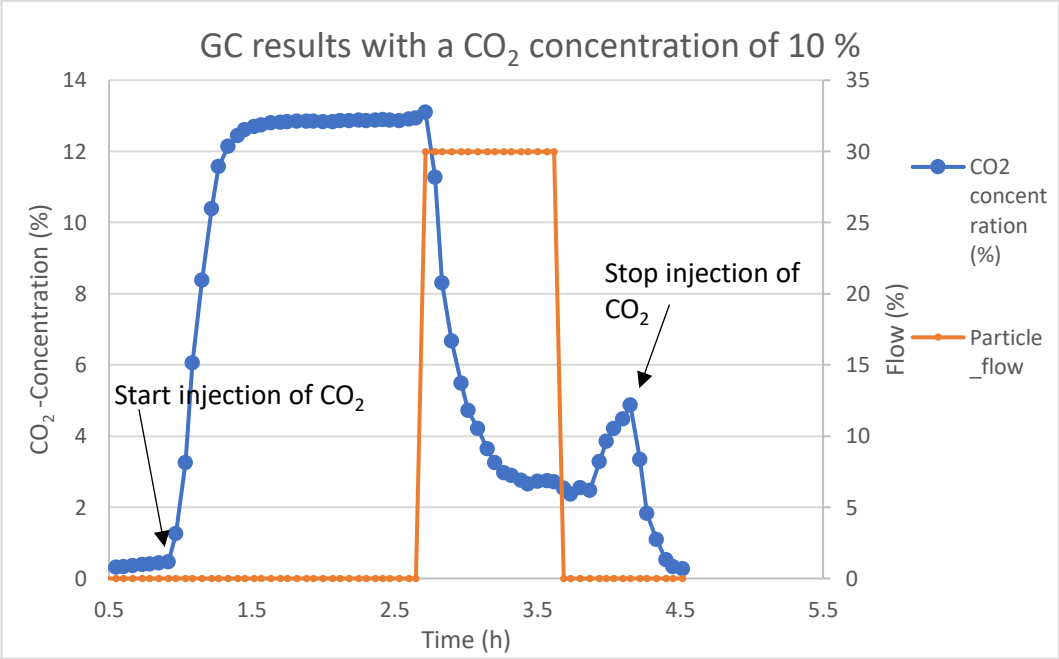

Figure 7.2 CO_2 concentration distribution during the test measured with the Micro-GC (08.09.2021)

The drop of the CO_2 concentration inside the reactor demonstrates that the reaction was taking place. The curve levels at 13 % (set concentration) and remains constant until the particles enter the system. Then, the curve drops, which signalizes that the CO_2 inside the air mixture decreases, which means that the CaO reacts with the CO_2 and forms $CaCO_3$. The concentration reaches almost 2 % at its optimum state. Once the particle flow stops, the concentration of CO_2 increases again since there aren't any particles left inside the reactor to react with the CO_2. All in all, the concentration drops from around 13 % to almost 2 % at the bottom of the curve. The efficiency of the system will be discussed in the following sections of this chapter.

Test: 10 % of CO_2 – 5 kg/h of CaO

Another test with the same CO_2 concentration as the test from above (13 %) was conducted, however the mass flow was modified from 7.8 – 5 kg/h, to observe the influence of the mass flow of the particles on the efficiency of the system. Other than the temperature distribution and the particle flow, the Figure 7.3 also displays the CO_2 concentration inside the reactor.

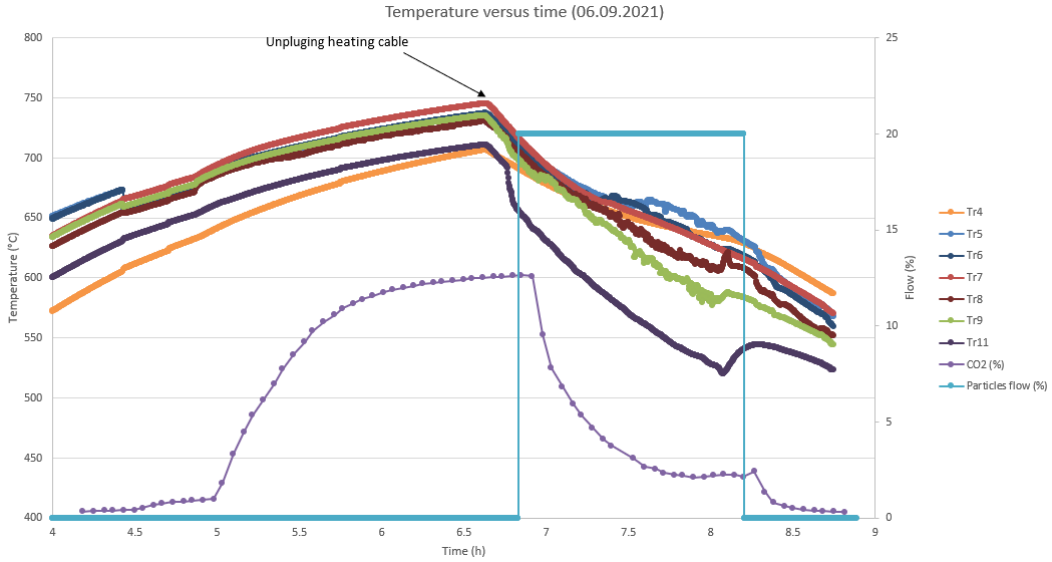

Figure 7.3 Temperature curves of thermocouples and particle flow and CO concentration over time with 10% CO_2 input (06.09.2021)

Once the particles enter the system, CaO and CO_2 react instantly, as the concentration inside the reactor drops drastically. From there the CO_2 concentration decreases in a slower manner, indicating a lower reaction rate. This can be explained due to the fact that at the beginning the gas mixture is exposed to only fresh particles, which react instantly. Over time, the reactor is filled with $CaCO_3$ particles. Furthermore, the carbonation reaction favors temperatures of around 650 – 700 °C. Lower temperatures lead to a lower reaction rate, which is also proven in the before studied TGA analysis. Within one hour, after the particle injection starts, around 100 °C of the temperature level drops. In summary, it can be said that the CO_2 concentration inside the reactor drops sharply, while being exposed to the ideal operation conditions of the CaL process. Once the temperature decreases, and the furnace is filled with non-fresh particles, the reaction rate shrinks as well.

7.2 Comparison Tr10

The carbonation reaction is known to be exothermic. For this reason, a temperature increase was expected, once the reaction is taking place, aiming to increase the general temperature inside the reactor. This might not be the case since the overall temperature inside the reactor seems to be the same as during the hot tests. However, looking closely at the temperature distribution curves, the line for the thermocouple Tr10 seems to be exceptional to the others. (Figure 7.4)

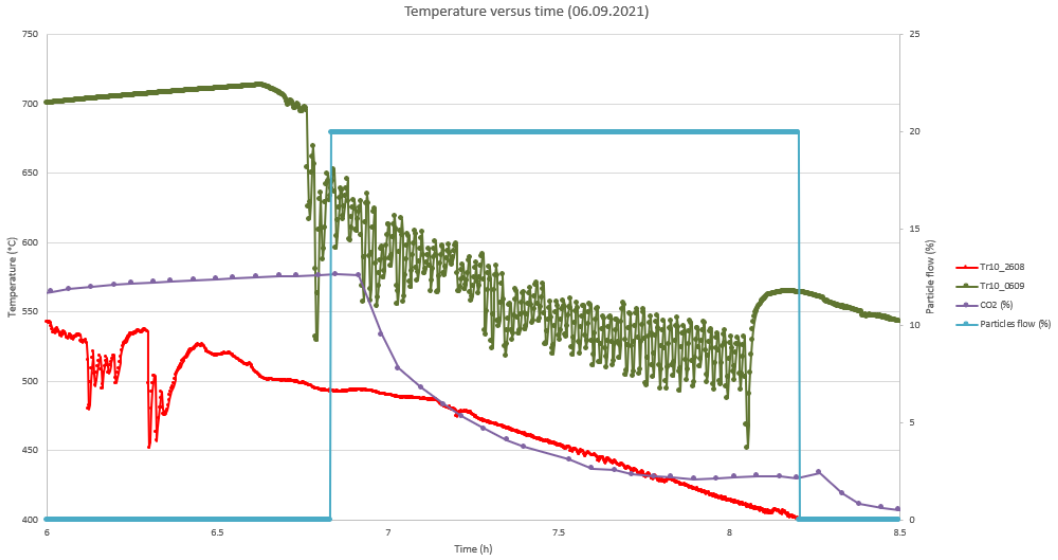

Figure 7.4 Temperature curve of thermocouple Tr10 and particle flow and CO_2 concentration over time (06.09.2021)

The green curve shows the temperature distribution of the thermocouple Tr10 on the 6th of September (chemical test), the red curve the temperature distribution on the 26th of August (hot test). A clear contrast is noticeable. While the curve from the hot test just decreases steadily, the curve from the chemical test fluctuates strongly during particle injection. Having a look on the other experimental results during the chemical tests, all the measurements for Tr10 seem to have the same tendency. In contrast, the same thermocouple shows a different behavior during the hot test, where no gas is yet injected to the system. The thermocouple is installed directly at the front part of the carbonator, where fresh particles enter the system and face the pure gas stream for the first time. The observed fluctuations might indicate that as measurable heat is emitted during the reaction.

Based on these peaks of maxima and minima, it might be true, that the fresh particles react instantly and release energy in form of heat. Since the number of particles and CO_2 is relatively low, the heat produced is not high enough to raise the general temperature level inside the carbonator, which is why the temperature drops again very quickly.

7.3 CO_2 efficiency

Finally, the systems efficiency can be assessed by regarding the CO_2 concentration development inside the reactor. Before having a look on the results, some marginal conditions for the limited particle injection phase should be clarified, since this might affect the efficiency of the system as well. Because the heating and cooling phase reactor require a lot of time, the injection phase of the particles was reduced to one hour. Another reason for the short injection time is the drop of the temperature inside the reactor once the cold particles enter the reactor. At some parts of the carbonator, the overall temperature (600 °C) is below the carbonation temperature (650 °C). This can be seen in Figure 7.3. While the temperature inside the reactor is still very high at the beginning of the injection phase, the concentration of the CO_2 inside the flue gas decreases drastically, indicating a successful reaction. As the temperature decreases acutely once the particles get injected, the CO_2 concentration inside the reactor stabilizes even to the point that the concentration increases again before the CO_2 supply is stopped.

To specify the efficiency of each test, the CO_2 concentration inside the reactor before and after must be compared. This can be done using the stochiometric equations and the conditions given in the Table 7.3.

The numbers are from the test of the 8th of September and shall be an example to present the outcome and the results.

Table 7.3 Data of the experimental set-up (08.09.2021)

Date	08.09.2021
Concentration CO_2 (%)	10 %
Airflow (l/min)	28 l/min
CO_2 flow (l/min)	3 l/min
Gas flow (l/min)	31 l/min
Particle flow (kg/h)	7.8 kg/h

A concentration of 10 % CO_2 was aimed. However, based on the GC-values the actual concentration initially is around 13.1 %. This is since the airflow fluctuates and the composition and a steady value cannot be hold during the whole process. The actual CO_2 flow can be calculated with a basic calculation using the CO_2 concentration at each measured point and the value of the gas flow.

The lowest CO_2 concentration is reached once the reaction takes place and is approximately 2.7 %. (Figure 7.5)

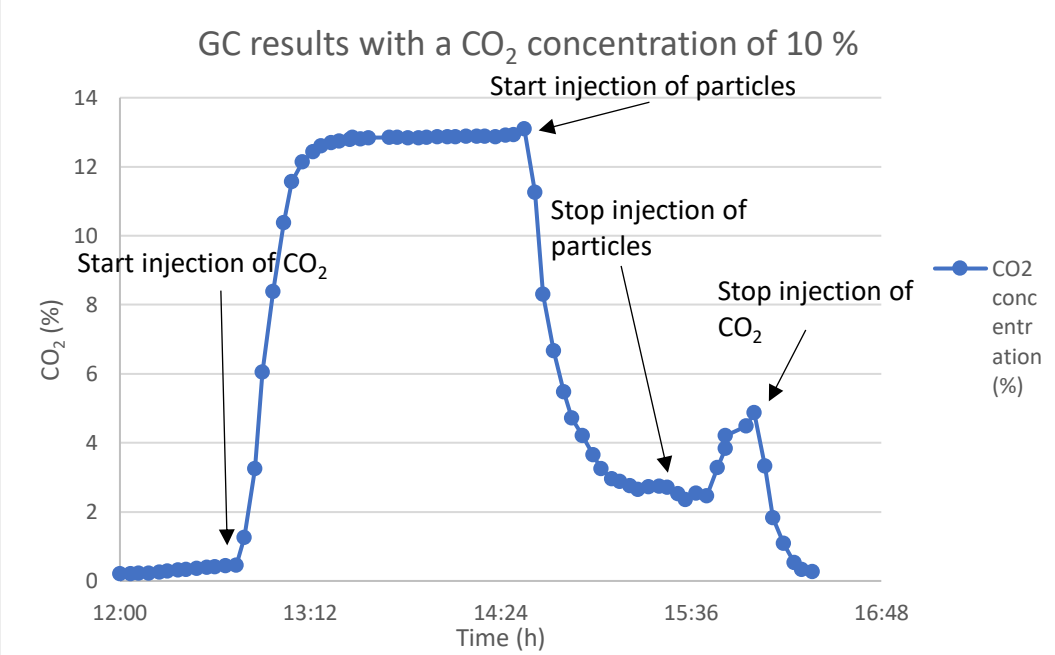

Figure 7.5 CO_2 concentration distribution during the test measured with the Micro-GC (08.09.2021)

In order to calculate the efficiency of the system at each point, the molar ratio of the substances is needed as well as other stochiometric values of the substances, and the results from the GC, which are all listed in the Table 7.4 below.

Table 7.4 Molar data for further calculation

Molar Mass CaO (g/mol)	56 g/mol
Molar Mass CO_2 (g/mol)	44 g/mol
Molar Volume CO_2 (l/mol)	22.4 l/mol
Volume flow @ 13.1 % CO_2 (l/min)	4.061 l/min
Volume flow @ 2.7 % CO_2 (l/min)	0.837 l/min

The efficiency of the whole system can be calculated with the following equation:

$$\frac{(\dot{n}_{initial} - \dot{n}_{end})}{\dot{n}_{initial}} * 100 \quad (4)$$

Where n equals the amount of mol at each point. The amount of mol can be calculated, using the molar volume of the substance as well as the volume flow. Based on these formulas, the following graph (Figure 7.6) can be plotted.

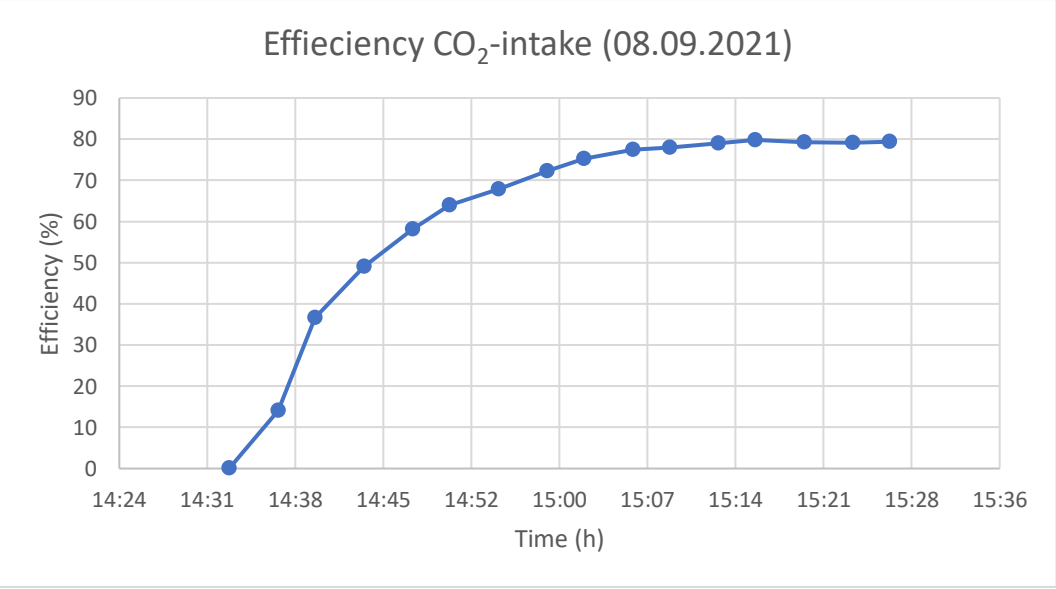

Figure 7.6 Efficiency of CO_2 intake over time (08.09.2021)

At first, the curve is increasing steeply, within the first 15 minutes, where 50 % of the CO_2 reacts with the CaO. During the next 45 minutes, the curve increases steadily, until reaching a saturation at the maximum of around 80 %. Concluding, an 80 % efficiency rate can be reached, when the flue gas consists of 10 % CO_2 and the mass flow of the particles amounts 7.8 kg/h.

This procedure can be repeated for every test, which were recorded to compare the numbers and draw conclusion about the ideal conditions to operate the carbonator. The Figure 7.7 visualizes the efficiency of different tests with different operation conditions.

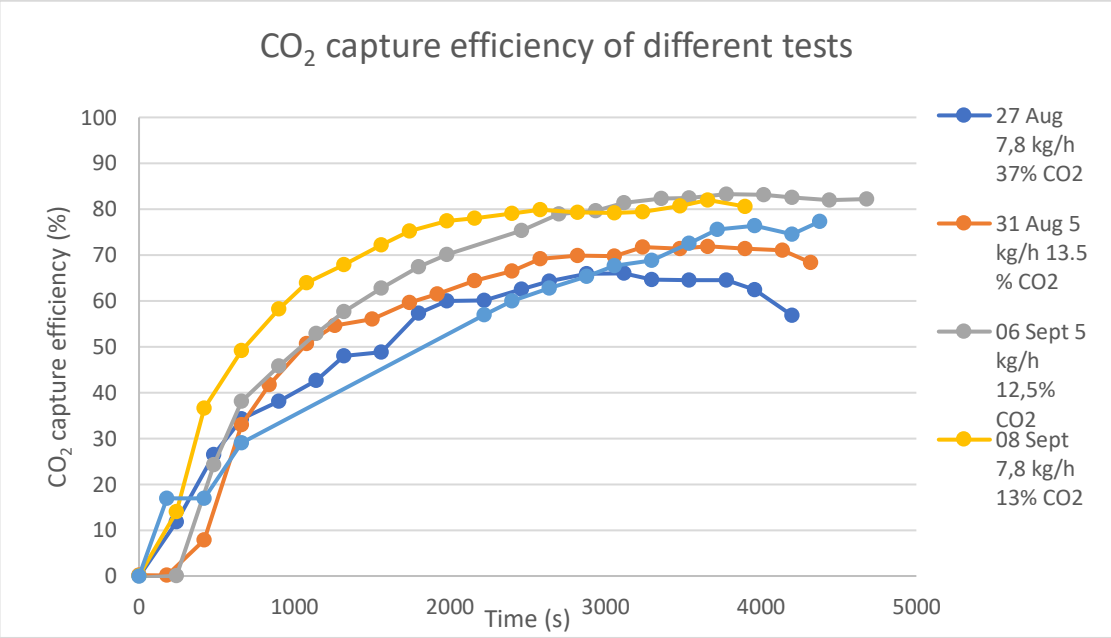

Figure 7.7 CO_2 capture efficiency of different tests

These curves present the recorded data during the tests. Each of them displays the CO_2 capture efficiency during a test run. Since the heating behavior of the carbonator was studied intensely in the previous tests before, an overall constant temperature was reached during all the chemical tests, with a deviation of +- 20 °C, and thus warrant an overall equal temperature. Before addressing the results, a few remarks should be mentioned.

As the carbonator and the system only started to operate for a short time before starting the chemical tests, some problems occurred within the test run and may have caused some falsified results as well as missing data.

The rotation of the reactor stopped during the test, the GC stopped recording data, and the particles kept sticking on the wall of the reactor. These issues helped in creating awareness over shortcomings of the experimental conduct that could be fixed and eventually lead to a better test run in the future. Nonetheless, the results which were obtained during all the tests are quite promising.

The carbonator reached an CO_2 capture efficiency of around 80 % maximally, which can be enhanced if the ideal operation conditions become more apparent.
It is clearly visible that the capture efficiency of the system favors at lower CO_2 concentrations. For lower concentrations the capture efficiency reaches more than 80 %, whereby at higher concentrations of CO_2 (30 %), the efficiency is at around 60 – 70 %. This can be explained by the fact that the same number of particles must capture double or even triple the quantity of CO_2 out of the flue gas. The increase of the mass flow of particles would lead to a higher capture efficiency respectively. However, having a look at the curves from the 6th of September (5 kg/h, 12.5 %) and 8th of September (7.8 kg/h, 13 %), a higher CO_2 capture would have been expected at a higher mass flow of particles, however this is not the case. (Figure 7.7)
As the CO_2 and particles injection part was reduced to one hour, the results may have differed, if a longer injection period would be possible. The curve from the 10th of September (7.8 kg/h, 26 %) could hint that this statement may be true, since the curve didn't reach saturation, but continues to increase, until the recording was stopped.
Another striking point is the difference of the efficiency of the tests on the 31st of August (5 kg/h, 13.5 %) and the 6th of September (5 kg/h, 12.5 %), carried out at the same conditions, however resulting to a capture efficiency of 70 % and above 80 %, which makes a difference of more than 10 %. (Figure 7.8)

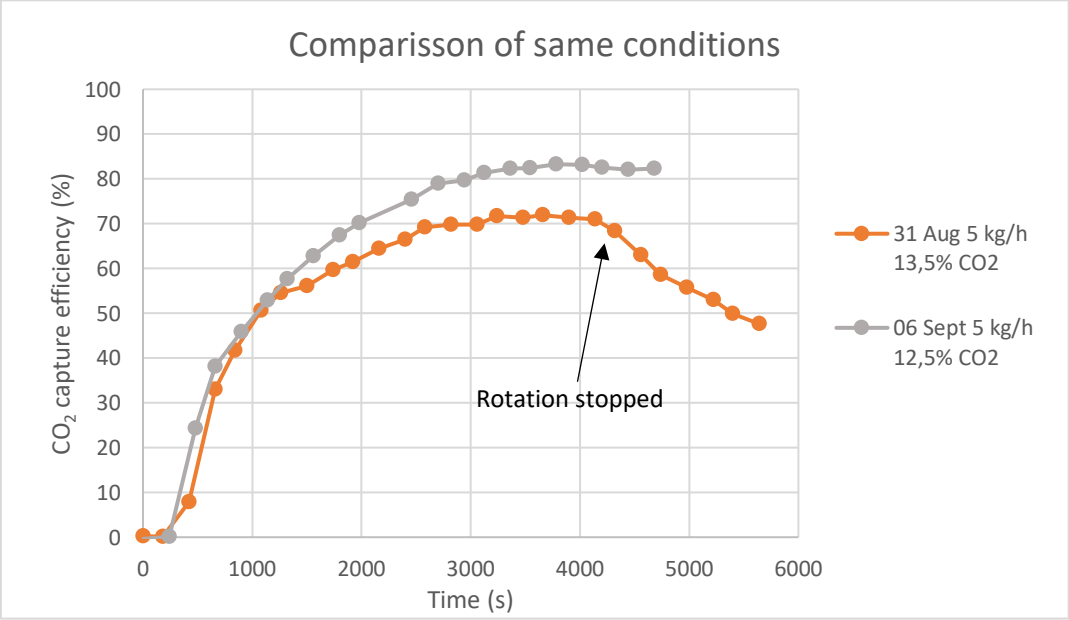

Figure 7.8 CO_2 capture efficiency of tests with the same conditions

The average temperature, the system reached during the whole injection phase for both tests, is between 640 – 650 °C, a nearly similar temperature distribution for both. This means, that the temperature difference is not the cause for the striking difference of the efficiency. Other than that, during the test from the 31st of August, the rotation of the reactor stopped within the injection phase of the particles at around 4000 seconds and thus the CO_2 concentration inside the reactor increased, after reaching an efficiency of around 70 %. Though the sudden rotation stop is also not the reason for the great difference, which is clearly visible when having a look on the curves and their development during the first 1000 seconds. Both curves start at a very similar course, until after 1000 seconds, where the gap evolves and widens over time. Furthermore, during the test from August there was slightly more CO_2 to capture than in the test from September, which could also result to the great capture difference. Other factors, which are inconspicuous, need to be observed and considered, for further tests in future and will be discussed later.

7.4 TGA results

To verify the reaction and specify the efficiency of the system, a re-reaction has to be conducted. If during the chemical tests, a reaction between the CaO and CO_2 took place, the product $CaCO_3$ must be present in the storage of the reactor. This can be confirmed by analyzing the material in the TGA. The re-reaction was executed at calcination temperature (1000 °C) to study the decarbonation reaction.

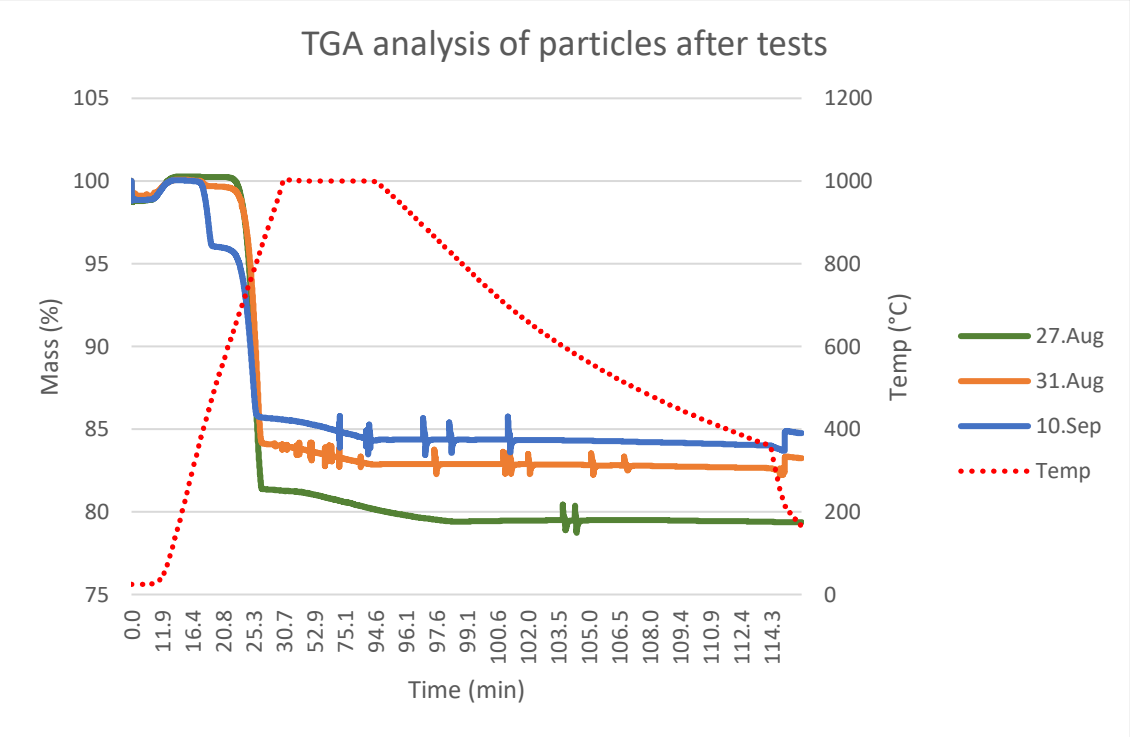

Figure 7.9 TGA results of particle analysis after going through carbonation

Based on the TGA results which were conducted on the particles inside the storage, the carbonation was successful and can be confirmed. The TGA was conducted on the particles, which went through the carbonator during the Chemical tests. 20 mg of these particles were placed in the TGA and went through a decarbonation test. During the test, the temperature inside the furnace was set to calcination temperature (1000 °C) and the mass change in percent was observed over time. The three curves of the Figure 7.9 show the particle analysis of the tests from the 27th of August (green), the 31st of August (orange), and the 10th of September (blue). All of them drop, once reaching a temperature of around 800 °C, indicating that CO_2 is released.

The test from the 27th of August has the highest reaction rate, as the curve drops from 100 % to around 78 %. This is due to the high CO_2 concentration input during the chemical test, which was around 37 %. Since the molar flow of CaO was higher than the corresponding molar flow of CO_2, the stochiometric ratio was not respected and so a reaction rate of 100 % cannot be expected. However, the results are really promising since the conversion of CaO is ranged between 27 – 46 %. (Table 7.5)

Table 7.5 Conversion rate of Cao for different experiments

	27th August	**31st August**	**10th September**
Reaction rate (%)	45.77	27.1	29.77

7.5 Difficulties and countermeasures for future projects

This chapter deals with the detailed clarification of the problems which occurred during the experimental campaign. Out of occasion countermeasures will be addressed.

As already mentioned before, CaO tends to absorb water out of the surrounding air and becomes denser and stickier. This caused difficulties while handling it during the experiments. The particles kept sticking at the walls of the reactor and created a growing layer on the inner wall. Instead of moving freely and facing the gas stream, are stagnant, leading to a decreased exposure to the gas and thus to a decreased reaction rate. Depending on the conditions of the day, whether the ambient atmosphere was dry or humid, the particles were either stickier or less, which was hard to control. For this reason, the reactor needed to be cleaned occasionally. This procedure consumed a day, since the whole cylinder needed to be demounted, the reactor transported to an open space, and the cleaning itself was time consuming. A clean reactor ensures a free movement inside the reactor, since the particles tend to stick less to the plane surface of the wall but rather to each other. This behavior was uncontrollable during the experiments and was only observed once the tests started.

There are several options to counteract this obstacle, e.g., choosing particles with a bigger grain size, reduce the exposure of the CaO to the surrounding air or dry the particles before using them. As already discussed in the earlier chapters, the particles size is responsible for its flow characteristics. Furthermore, any direct exposure to the surrounding air must be avoided, cause CaO absorbs moisture out of the surrounding air. It needs to be stored airtight all the time, even in the storage of the screw feeder. Drying the particles, before injecting them into the reactor could improve the flow behavior and raise the temperature of the particles. Raising the temperature of the particles would also benefit the difficulty with the temperature drop once the particles enter the system. Within one hour, the average temperature inside the reactor drops almost an amount of 100 °C. Based on the recorded data, it is visible the reaction stops, once the average temperature inside the furnace is below the carbonation temperature. In Figure 7.3, there is a hint that the CO_2 concentration is going to rise slightly, after reaching a constant value. A higher efficiency of the system could be ensured if the temperature drop wouldn't be so significant. The idea of preheating the particles, before injecting them into the reactor, could be a key action. For this, a system must be developed, connecting the heating facility with the screw feeder.

Furthermore, the bearing of the carbonator caused a few issues. Due to the forces, which were constantly acting on the bearing, it wore out faster than expected. After already 3 – 4 test runs, the carbonator leaked gas, thus the system had to be tightened again, by fixing the screws. After about 4 – 5 test runs, the bearing wore of completely and needed to be replaced by a new one. Usually, replacing the bearing and cleaning the reactor was combined. Anyway, replacing the bearing all the time, is not the ideal option, therefore, a bearing with better glide properties, which can withstand the high temperatures as well, needs to be chosen. Since two planar surfaces are constantly in touch with the bearing and exert a huge force on the bearing, wear is always guaranteed, therefore a new idea for the bearing is also an option for the carbonator, to make it applicable in future.

Apart from these hardships, the design and the implementation of the carbonator was proven to be already successful, aiming to become optimal in further operation.

8 Summary and Outlook

The calcium looping cycle, for the extraction of CO_2 from CO_2 rich flue gases has been demonstrated for several decades. For now this is only in its pilot stage, though offering significant potential for reduction of greenhouse gas emissions from industrial power plants. While few projects achieved the implementation of carbonators and calciners as retrofits in existing power plants, the urge for innovative and effective implementations is still omnipresent. This project and thus this thesis contribute to the development of a new kind of carbonator, giving insight about its basic design and modelling, the process parametric studies and its efficiency as its serves as a model and example for further rotary kiln carbonator reactors.

8.1 Summary

The calcium looping cycle is a promising carbon capture technology making use of the reversible carbonation/calcination cycle, whereby the carbonation reaction has been demonstrated in the carbonator reactor during the project of this thesis. The whole work concentrated on three main tasks. First, validating the design of the carbonator and the required components to build the carbonator and later set it up for the experimental campaign. Second, investigating the operational parameters through analysis of the stochiometric balance and TGA analysis, followed by an experimental campaign. And last, validating the parameters and thus efficiency of the system during the ongoing experimental campaign.

The calcium looping process is based on the reversible carbonation of a CaO-based sorbent, when reaching a temperature of about 650 – 700 °C. The idea is that CaO extracts CO_2 out of CO_2 rich flue gases. This scenario was demonstrated during this project. For this purpose, a rotary kiln carbonator was designed and set up.

Everything started with validating the design of the carbonator and procuring the missing components. Simultaneously the carbonator was mounted together, which consists of various individual parts. Once the carbonator was set up, the experimental set-up was realized. Before running the experimental campaign, essential parameters for the carbonation reaction for a rotary kiln reactor needed to be determined and clarified.

These are: the temperature distribution inside the furnace, the residence time of particles and the gas mixture, and the concentration of CO_2 inside the gas mixture and the volume flow of it, as well as other parameters that cannot be influenced. A TGA analysis was conducted on the CaO material, which were used for the experiments. The TGA gave information about the minimal required time to start the carbonation reaction as well as a reference value for the residence time for a complete carbonation of the material. Based on the information from the TGA, a volume flow for the gas mixture was estimated.

Several cold & hot tests were conducted, to adjust the components used and acquire knowledge about the behavior of certain components. During the cold tests, the motors used, screw feeder and CO_2-sensor were calibrated. Moreover, the ideal settings were adjusted during the cold tests. The residence time depends on the rotational velocity of the reactor, the mass flow of the particles, and the angle of inclination of the carbonator. These three were coordinated accordingly, to achieve the required residence time. The hot tests were conducted to acquire knowledge about the heating behavior of the whole system to be able to predict the required time, to raise the whole system to a specific temperature level.

Cold and hot tests delivered the required information and knowledge to conduct the chemical tests and start the experimental campaign to estimate the operability and efficiency of the system. The overall aim of this project was not to reach highest possible reaction rate of the carbonation but a high CO_2 capture efficiency out of the flue gas flow. Since time was limited, and some parameters were already predefined through the grain scale study, the focus during the experimental campaign was on the adjustment of the CO_2 concentration inside the gas mixture and mass flow of particles, to achieve the highest possible capture efficiency of the particles.

Overall, a CO_2 capture efficiency of maximal 83 % was reached for the test on the 6^{th} of September with a mass flow of 5 kg/h and a CO_2 concentration of 12,5%. The overall capture efficiency of all tests was around 60 – 80 %, which is already really promising, since the testing period was limited to a very short time span, and the test in the carbonator were conducted for the very first time. Generally, it can be said that the capture efficiency is the largest, if the mass flow is set higher and the CO_2 concentration is set lower, while keeping the suitable residence time in mind.

Since the time was limited, and only a few tests were conducted, no clear regularity is yet observable, but an approximate tendency is noticeable. In conclusion, promising results showcased the operability of the new kind of carbonator reactor, with high capture efficiencies.

Limitations of the lab-scale facility became apparent during the operation. These limitations are the great drop of the overall temperature inside the reactor, leading to a lower capture efficiency, the stickiness of the material, making it hard to handle during the experiments, and the limit of the bearing. In addition, some suggestions were discussed: Such as preheating the particles before injecting them, to avoid the drastic temperature drop, rethinking the choice of particles again, to ensure a better flow property, and to find a better solution for the bearing of the reactor, since the implemented one wears off after only a few test runs.

8.2 Outlook

The sustainable development of a low CO_2 emission strategy may be achieved with calcium looping. For studying the calcium looping process, a lab-scale rotary kiln carbonator was set up and tested within the projects run time, where capture efficiencies of more than 80 % were achieved with the possibility to reach an even higher efficiency.

As time was limited during the project, the experimental campaign was limited to a short amount of test runs and to a limit of two variable parameters, which are the particle flow and the CO_2 concentration of the gas mixture. Conducting more experiments and experimenting with the fixed parameters, namely the residence time of particles, the volume flow of the gas mixture eventually could lead to even higher efficiencies of the system.

The temperature inside the reactor is not controllable. When injecting the particles, the temperature level inside the reactor drops drastically, indirectly determining the injection time. It may be possible that higher efficiencies could have been reached if the injection time is not limited to one hour. As before mentioned, preheating the particles could be a way to counteract and adjust the insulation to reduce the heat loses.

9 References

References

[1] IEA, International Energy Agency, “Net Zero by 2050 - A Roadmap for the Global Energy Sector,” 2021.

[2] IEA - International Enery Agency, “Phasing Out Unabated Coal: Current Status and Three Case Studies,” 2021.

[3] J. Friedmann, *Julio Explains It All: Why We Need Carbon Capture for Climate.* [Online]. Available: https://www.thirdway.org/video/julio-explains-it-all-why-we-need-carbon-capture-for-climate (accessed: Jul. 10 2022).

[4] P. Tilak and M. M. El-Halwagi, “Process integration of Calcium Looping with industrial plants for monetizing CO2 into value-added products,” *Carbon Resources Conversion*, vol. 1, no. 2, pp. 191–199, 2018, doi: 10.1016/j.crcon.2018.07.004.

[5] N. Rodríguez, R. Murillo, and J. C. Abanades, “CO_2 capture from cement plants using oxyfired precalcination and/or calcium looping,” *Environmental science & technology*, vol. 46, no. 4, pp. 2460–2466, 2012, doi: 10.1021/es2030593.

[6] M. Fischedick, K. Görner, and M. Thomeczek, *CO2: Abtrennung, Speicherung, Nutzung*. Berlin, Heidelberg: Springer Berlin Heidelberg, 2015.

[7] T. Hirama, H. Hosoda, K. Kitano, and T. Shimizu, “Method of Seperating carbon dioxide from carbon dioxide containing gas and combustion apparatus having function to seperate carbon dioxide from the combustion gas,”

[8] T. Shimizu, T. Hirama, H. Hosoda, K. Kitano, and M. Inagaki, “A Twin Fluid-Bed Reactor for Removal of CO2 from Combustion Processes,” *Chemical Engineering Research and Design*, vol. 77, pp. 62–68, 1999.

[9] D. P. Hanak, S. Michalski, and V. Manovic, “From post-combustion carbon capture to sorption-enhanced hydrogen production: A state-of-the-art review of carbonate looping process feasibility,” *Energy Conversion and Management*, vol. 177, pp. 428–452, 2018, doi: 10.1016/j.enconman.2018.09.058.

[10] J. C. Abanades, M. Alonso, N. Rodríguez, B. González, G. Grasa, and R. Murillo, “Capturing CO2 from combustion flue gases with a carbonation calcination loop. Experimental results and process development,” *Energy*

Procedia, vol. 1, no. 1, pp. 1147–1154, 2009, doi: 10.1016/j.egypro.2009.01.151.

[11] A. Charitos *et al.,* "Parametric investigation of the calcium looping process for CO2 capture in a 10kWth dual fluidized bed," *International Journal of Greenhouse Gas Control*, vol. 4, no. 5, pp. 776–784, 2010, doi: 10.1016/j.ijggc.2010.04.009.

[12] C. Hawthorne *et al.,* "CO2 capture with CaO in a 200 kWth dual fluidized bed pilot plant," *Energy Procedia*, vol. 4, pp. 441–448, 2011, doi: 10.1016/j.egypro.2011.01.073.

[13] SCARLET, "Scale-up of Calcium Carbonate Looping Technology for Efficient CO2 Capture from Power and Industrial Plants," 2017.

[14] M. Fantinia *et al.,* "Calcium Looping technology demonstration in industrial environment: status of the CLEANKER pilot plant," 2021.

[15] B. J. McBride, M. J. Zehe, and S. Gordon, "NASA Glenn Coefficients for Calculating Thermodynamic Properties of Individual Species," 2002.

[16] A. Silaban and D. P. Harrison, "High temperature capture of Carbon Dioxide: Characteristics of the reversible reaction between CaO(s) and CO2(g)," *Chemical Engineering Communications*, vol. 137, no. 1, pp. 177–190, 1995, doi: 10.1080/00986449508936375.

[17] J. Blamey, C. C. Dean, N. H. Florin, M. J. Al-Jeboori, and P. S. Fennell, "The calcium looping cycle for CO2 capture from power generation, cement manufacture and hydrogen production," *Chemical Engineering Research and Design*, vol. 89, no. 6, pp. 836–855, 2011, doi: 10.1016/j.cherd.2010.10.013.

[18] K. Labus, "Comparison of the Properties of Natural Sorbents for the Calcium Looping Process," *Materials (Basel, Switzerland)*, vol. 14, no. 3, 2021, doi: 10.3390/ma14030548.

[19] W. Reschetilowski, *Handbuch Chemische Reaktoren*. Berlin, Heidelberg: Springer Berlin Heidelberg, 2020.

[20] N. Rodríguez, M. Alonso, and J. C. Abanades, "Experimental investigation of a circulating fluidized-bed reactor to capture CO2 with CaO," *AIChE J.*, vol. 57, no. 5, pp. 1356–1366, 2011, doi: 10.1002/aic.12337.

[21] J. Kremer, A. Galloy, J. Ströhle, and B. Epple, "Continuous CO 2 Capture in a 1-MW th Carbonate Looping Pilot Plant," *Chem. Eng. Technol.*, vol. 36, no. 9, pp. 1518–1524, 2013, doi: 10.1002/ceat.201300084.

[22] J. Plou, I. Martínez, G. S. Grasa, and R. Murillo, "Experimental carbonation of CaO in an entrained flow reactor," *React. Chem. Eng.*, vol. 4, no. 5, pp. 899–908, 2019, doi: 10.1039/C9RE00015A.

[23] S. Turrado, B. Arias, J. R. Fernandez, and J. C. Abanades, "Carbonation of Fine CaO Particles in a Drop Tube Reactor," 2018.

[24] S. Abanades and L. André, "Design and demonstration of a high temperature solar-heated rotary tube reactor for continuous particles calcination," *Applied Energy*, vol. 212, pp. 1310–1320, 2018, doi: 10.1016/j.apenergy.2018.01.019.

Appendix A

Stochiometric balance of the carbonation reaction

Assumptions:		
Mass flow CaO:	5	kg/h
Concentration CO_2:	20	%
1. Reaction equation:		
$CaO+CO_2 = CaCO_3$		
2. Calculation molar mass M:		
Molar mass Ca:	40.078	g/mol
Molar mass O:	15.999	g/mol
Molar mass C:	12.011	g/mol
$M(CaO)+M(CO_2) = M(CaCO_3)$		
$M(CaO)= M(Ca)+M(O)$	56.077	g/mol
$M(CO_2)= M(C)+M(O_2)$	44.009	g/mol
$M(CaCO_3)$	100.086	g/mol
3. Calculation amount of substance n:		
Substance ratio of 1:1		
n= m/M		
Assumption 5000g CaO	5000	G
n= m/M		
n(CaO)	89.163115	Mol
$n(CO_2)$	89.163115	Mol
4. Calculation mass CO_2:		
m= n*M		
$m(CO_2)$	3923.97953	G
5. Calculation mass flue gas:		
20% dissolved in gas mixture	19619.8976	g
mass flow in one hour	19.6198976	kg/h
6. Volume flow of the gas:		

$$\dot{m} = \rho * \dot{V} \qquad \dot{V} = \frac{\dot{m}}{\rho}$$

Density of air		
$\rho(20°C)$	1.98	kg/m³
$\rho(700°C)$	0.3576	kg/m³
$\dot{V}(20°C)$	165.150654	l/min
$\dot{V}(700°C)$	914.42476	l/min